NACA TN 2455

NATIONAL ADVISORY COMMITTEE FOR AERONAUTICS

TECHNICAL NOTE 2455

A METHOD OF DESIGNING TURBOMACHINE BLADES WITH A DESIRABLE THICKNESS DISTRIBUTION FOR COMPRESSIBLE FLOW ALONG AN ARBITRARY STREAM FILAMENT OF REVOLUTION

By Chung-Hua Wu and Curtis A. Brown

Lewis Flight Propulsion Laboratory
Cleveland, Ohio

Washington

September 1951

1

NATIONAL ADVISORY COMMITTEE FOR AERONAUTICS

TECHNICAL NOTE 2455

2223

A METHOD OF DESIGNING TURBOMACHINE BLADES WITH A DESIRABLE THICKNESS DISTRIBUTION FOR COMPRESSIBLE FLOW ALONG AN ARBITRARY STREAM FILAMENT OF REVOLUTION

By Chung-Hua Wu and Curtis A. Brown

SUMMARY

A rapid method for designing turbomachine blades of a given turning and a desirable blade-thickness distribution for a compressible non-viscous fluid flow along an arbitrary stream filament of revolution is presented. The method utilizes the guiding effects of the blade shape on the mean streamline shape and of the blade thickness on the specific mass flow along the mean streamline. After the flow on the mean streamline is determined, the extension of the solution from the mean streamline to the blade surfaces is accomplished by the use of a power series. A number of blade profiles are obtainable for the total mass-flow requirement, and one is chosen for the best velocity distribution on the blade. The results obtained in the solution can be used for a direct check on the accuracy of series approximation and, also, for the more accurate determination of the velocity distribution along the leading and trailing edges of the blade.

The method is illustrated with the design of several turbine cascades of highly cambered thick blades. The determination of the shape of the blades and the compressible flow past the blades was carried out by hand computation in 16 hours. One solution obtained by using three terms in the power series compared very well with an available direct solution and the blade circulation checks closely the specified turning angle.

Because the surface of revolution, on which the blades are located, is completely arbitrary, the method can be applied to axial-flow, radial-flow, and mixed-flow turbomachines. The variation in the normal distance between the stream surfaces of revolution can be taken into account, thus incorporating into the design the principal effect of three-dimensional flow. The method is readily applied to the design of channels on a plane and on a general surface of revolution.

INTRODUCTION

The increasing use of compressors and turbines in aircraft power plants during the past 10 years has led to considerable research in the direct and inverse problems of two-dimensional potential flow past an infinite cascade of airfoils. In the inverse problem, the design of blades is often directed at control of the pressure or velocity distribution on the blade. Most of the methods are derived for axial-type turbomachines, in which the flow is assumed to take place on cylindrical surfaces (methods for incompressible and compressible flow are discussed in references 1 to 7 and 8 to 11, respectively). Methods for designing blades in a radial plane are given in references 12 and 10.

In current axial- and radial-flow turbomachines, the flow surfaces are usually of a more general shape than either cylindrical or radial. Furthermore, the normal distance between adjacent flow surfaces varies along the flow path. A method was therefore developed at the Lewis laboratory for the design of blades for compressible flow along an arbitrary stream filament of revolution. Instead of the velocity distribution on the blade being the required result, the blade design is aimed at a desirable blade-thickness distribution required with respect to blade strength and Mach number in general and also the coolant passage requirement in the case of cooled turbine blades. The computation involved in this method is relatively simple and short, and the usual assumption of a linear pressure-volume relation for compressible flow is not required.

For clarity and simplicity the method will first be given for compressible flow on a plane or a cylindrical surface and will be illustrated by a few examples. The method will then be given for the general case of compressible flow along an arbitrary stream filament of revolution.

2223

SYMBOLS

The following symbols are used in this report:

B differentiation coefficient

H total enthalpy, $h + \frac{1}{2} V^2$

H_w relative total enthalpy, $h + \frac{1}{2} W^2$

h static enthalpy

2223

I $h + \frac{1}{2} W^2 - \frac{1}{2} \omega^2 r^2$

L blade length projected on turbomachine axis

l, φ orthogonal coordinates on mean surface of revolution

M mass flow

P pitch or spacing

p static pressure of gas

r radial distance from axis of turbomachine

S streamline

t blade thickness in circumferential direction

V absolute velocity of gas

W velocity of gas relative to blade

y distance in direction of pitch for plane flow and equal to $r\varphi$ for flow on cylindrical surface

z distance along axis of turbomachine

β flow angle on stream surface, $\tan^{-1} \frac{W_y}{W_z}$ or $\tan^{-1} \frac{W_\varphi}{W_l}$

ρ density of gas

σ angle between tangent to meridional curve and axis, $\tan^{-1} \frac{W_r}{W_z}$

τ normal thickness of stream filament of revolution

γ ratio of specific heats

ψ stream function

ω angular velocity of blade

Superscript:

$*$ dimensionless value

Subscripts:

e	exit
i	inlet
l,φ	meridional and circumferential components
m	mean streamline
p	pressure surface of blade
s	suction surface of blade
T	total or stagnation state
y	y-component
z	z-component

2223

DESIGNING BLADES FOR COMPRESSIBLE FLOW IN PLANE OR ON CYLINDRICAL SURFACE

General Description of Method

In a recent investigation of compressible flow through a typical cascade of turbine blades (reference 13), the following results were obtained:

(1) The shape of the mean streamline follows approximately that of the mean channel line of the cascade and has a lower curvature.

(2) The variation of the ratio of the specific mass flow on the mean streamline to its inlet value follows the trend in the variation of the ratio of pitch to channel width (inside the channel the ratio of the specific mass flow is about 4 percent greater than the ratio of pitch to channel width).

(3) The variation in fluid properties across the channel can be represented by a second-degree function for engineering accuracy.

These results were used herein to develop a rapid method for designing cascade blades for either compressible or incompressible flow.

This method of blade design starts with the calculation of the compressible flow on the mean streamline. With the flow angle upstream

and downstream of the blade determined by the velocity diagram and the pitch and the axial length of the blade given, a particular mean streamline shape may be sketched by the designer. The designer may use the shape of the mean streamline itself as a parameter of the cascade or may specify the mean streamline shape according to figure 17 or reference 13 (or even better according to any available relation of a similar blading) to lead to a certain blade camber line. (If only a number of points of this streamline are specified, it is important that the values given are numerically smooth). In addition to the mean streamline shape the designer further specifies at a finite number of points along the mean streamline (such as $z_1 \ldots z_{18}$ in fig. 1), the ratio of specific mass flow on the mean streamline to inlet value. The values of the specific mass flow on the mean streamline are determined by the blade-thickness distribution which is desirable from the consideration of blade stress and Mach number in general, and the consideration of the additional requirement of coolant passage in the case of cooled turbine blades, and by a relation between blade-thickness distribution and specific mass flow on the mean streamline, such as shown in figure 19 of reference 13.

2223

With these specified values, the velocity components and the density are very easily determined at the specified points on the mean streamline. The variation of velocity components and density in the pitch direction are then obtained by using power series in that direction. The derivatives in the series are determined from the fluid state on the mean streamline by the use of equations of continuity and motion and the density-velocity relation for isentropic flow. A number of blade profiles and their velocity distributions are obtained by interpreting the starting mean streamline as dividing the inlet mass flow into two slightly different amounts in the channel. The velocity distributions on the blades are compared and the best one is chosen. If the blade shape, the thickness distribution, or the velocity distribution around the blade obtained requires some modification, the values specified for the mean streamline should be modified and the process repeated. Because of the relatively short computation involved (in the illustrative examples of turbine blades, only 16 hours were required for the compressible solution by using the first three terms in the series and 6 to 10 stations inside the channel), modifications of the solution for more desirable blade thickness or velocity distribution is practical. Families of blade elements can be built up very quickly this way for any particular application.

Basic Relations

The steady two-dimensional isentropic flow of a nonviscous fluid in a plane or on a cylindrical surface is governed by the following equations of continuity and irrotational motion, and the isentropic pressure-density relation:

$$\frac{\partial(\rho W_z)}{\partial z} + \frac{\partial(\rho W_y)}{\partial y} = 0 \tag{1}$$

$$\frac{\partial W_z}{\partial y} - \frac{\partial W_y}{\partial z} = 0 \tag{2}$$

$$p = K\rho^{\gamma} \tag{3}$$

In these equations, the z coordinate is chosen along the machine axis and the y coordinate is chosen along the pitch direction ($y = r\varphi$ in the case of cylindrical flow with r equal to a constant).

2223

Consider first the gas flow along a streamline somewhere in the midpart of the channel formed by two neighboring blades, such as ab in figure 1. The coordinates of the streamline and their differentials are related, respectively, by the following two equations:

$$S(z,y) = 0 \tag{4}$$

$$\frac{\partial S}{\partial z}\,dz + \frac{\partial S}{\partial y}\,dy = 0 \tag{5}$$

When the variation of the fluid state along the streamline is considered, any quantity q on the streamline is a function of z only, that is,

$$q = q\left[z, y(z)\right] \tag{6}$$

The total derivative of q with respect to z is

$$\frac{dq}{dz} = \frac{\partial q}{\partial z} + \frac{\partial q}{\partial y}\frac{dy}{dz} \tag{7}$$

But

$$\frac{dy}{dz} = -\frac{\dfrac{\partial S}{\partial z}}{\dfrac{\partial S}{\partial y}} = \frac{W_y}{W_z} = \tan\beta \tag{8}$$

Hence equation (7) may be written as

$$\frac{dq}{dz} = \frac{\partial q}{\partial z} + \tan\beta\,\frac{\partial q}{\partial y} \tag{9}$$

When equation (9) is used, the continuity and irrotationality relations can be written as

$$\frac{d(\rho W_z)}{dz} - \tan\beta \frac{\partial(\rho W_z)}{\partial y} + \frac{\partial(\rho W_y)}{\partial y} = 0 \tag{10}$$

and

$$\frac{dW_y}{dz} - \frac{\partial W_z}{\partial y} - \tan\beta \frac{\partial W_y}{\partial y} = 0 \tag{11}$$

2223

The variation of density throughout the flow region can be most conveniently expressed in terms of its inlet value through the use of equation (3) as follows:

$$\rho^* = \frac{\rho}{\rho_i} = \frac{\rho_{T,i}}{\rho_i} \frac{\rho}{\rho_{T,i}} = \frac{\rho_{T,i}}{\rho_i} \left(1 - \frac{W^2}{2H_w}\right)^{\frac{1}{\gamma-1}} \tag{12}$$

A tabulated general relation of $\rho/\rho_{T,i}$ in equal intervals of W^2/H_w can first be calculated, from which either a table for ρ/ρ_i in equal intervals of W^2 or a graph can be easily constructed for each individual case and used for the evaluation of density from the velocity.

Along the chosen (mean) streamline, where the slope is known and ρW_z is given at a number of stations, the density at these stations can be obtained as follows: Rewrite equation (12) as

$$\rho^* = \frac{\rho}{\rho_i} = \left[\frac{1 - \frac{W_{z,i}^2}{2H_w\rho^{*2}} (\rho^* W_z^* \sec\beta)^2}{1 - \frac{W_i^2}{2H_w}}\right]^{\frac{1}{\gamma-1}} \tag{12a}$$

or

$$(\rho^* W_z^* \sec\beta)^2 = 2 \frac{H_w \rho^{*2}}{W_{z,i}^2} \left[1 - (\rho^*)^{(\gamma-1)} \left(1 - \frac{W_i^2}{2H_w}\right)\right] \tag{12b}$$

where

$$W_z^* = \frac{W_z}{W_{z,i}}$$

Either equation (12a) is used to prepare a table of ρ^* for equal intervals of $(\rho^* W_z^* \sec \beta)$ by an iterative process, or equation (12b) is used to compute $\rho^* W_z^* \sec \beta$ for a number of values ρ^*, which are then plotted as a graph. After densities have been obtained from either a table or graph, the velocity components on the chosen (mean) streamline are readily computed. The fluid state is then extended out in the pitch direction by the equations given in the next section (compare with references 14 and 15).

2223

Variation of Fluid State in Pitch Direction

Equations (8), (10), (11), and (12) directly give the first-order partial derivatives of W_z, W_y, and ρ with respect to y in terms of the known quantities on the chosen (mean) streamline as follows:

$$\frac{\partial W_z}{\partial y} = \left[\frac{dW_y}{dz} + \tan \beta \, \frac{1}{\rho} \frac{d(\rho W_z)}{dz}\right] \cos^2 \beta \tag{13}$$

$$\frac{\partial W_y}{\partial y} = \left[\tan \beta \, \frac{dW_y}{dz} - \frac{1}{\rho} \frac{d(\rho W_z)}{dz}\right] \cos^2 \beta \tag{14}$$

$$\frac{1}{\rho} \frac{\partial \rho}{\partial y} = - \frac{1}{(\gamma - 1)\left(H_w - \frac{W^2}{2}\right)} \left(W_z \frac{\partial W_z}{\partial y} + W_y \frac{\partial W_y}{\partial y}\right) \tag{15}$$

The second-order partial derivatives of W_z, W_y, and ρ with respect to y can be obtained as follows: Differentiating the continuity equation (1) with respect to y results in

$$\frac{\partial^2 (\rho W_z)}{\partial z \, \partial y} + \frac{\partial^2 (\rho W_y)}{\partial y^2} = 0 \tag{16}$$

Equation (16) can be written through the use of relation (9) as

$$\frac{\partial^2 (\rho W_y)}{\partial y^2} - \tan \beta \, \frac{\partial^2 (\rho W_z)}{\partial y^2} + \frac{d}{dz} \frac{\partial (\rho W_z)}{\partial y} = 0 \tag{17}$$

which is expanded to obtain

$$\rho \frac{\partial^2 W_y}{\partial y^2} + 2 \frac{\partial \rho}{\partial y} \frac{\partial W_y}{\partial y} - \left(\rho \frac{\partial^2 W_z}{\partial y^2} + 2 \frac{\partial \rho}{\partial y} \frac{\partial W_z}{\partial y}\right) \tan \beta + \frac{d}{dz} \frac{\partial (\rho W_z)}{\partial y} = 0 \tag{18}$$

From equation (10)

$$\frac{\partial W_y}{\partial y} = \tan \beta \frac{\partial W_z}{\partial y} - \frac{1}{\rho} \frac{d(\rho W_z)}{dz} \tag{19}$$

Differentiating the irrotationality equation (2) with respect to y and using equation (9) yield

$$\frac{\partial^2 W_z}{\partial y^2} = \frac{d}{dz} \frac{\partial W_y}{\partial y} - \tan \beta \frac{\partial^2 W_y}{\partial y^2} \tag{20}$$

Substituting equations (19) and (20) into equation (18) results in

$$\rho \frac{\partial^2 W_y}{\partial y^2} - \frac{2}{\rho} \frac{d(\rho W_z)}{dz} \frac{\partial \rho}{\partial y} - \rho \left(\frac{d}{dz} \frac{\partial W_y}{\partial y} - \tan \beta \frac{\partial^2 W_y}{\partial y^2} \right) \tan \beta + \frac{d}{dz} \frac{\partial (\rho W_z)}{\partial y} = 0$$

Transposing and combining terms give

$$\frac{\partial^2 W_y}{\partial y^2} = \left[\frac{2}{\rho^2} \frac{d(\rho W_z)}{dz} \frac{\partial \rho}{\partial y} - \frac{1}{\rho} \frac{d}{dz} \left(\rho \frac{\partial W_z}{\partial y} + W_z \frac{\partial \rho}{\partial y} \right) + \tan \beta \frac{d}{dz} \frac{\partial W_y}{\partial y} \right] \cos^2 \beta \tag{21}$$

After this equation is evaluated, the second partial derivative of W_z with respect to y is obtained by using equation (20):

$$\frac{\partial^2 W_z}{\partial y^2} = \frac{d}{dz} \frac{\partial W_y}{\partial y} - \tan \beta \frac{\partial^2 W_y}{\partial y^2} \tag{22}$$

A typical computation for these derivatives is presented in tables I and II.

The second-order partial derivative of ρ with respect to y is obtained again from equation (12):

$$\frac{1}{\rho} \frac{\partial^2 \rho}{\partial y^2} = \frac{2-\gamma}{\rho^2} \left(\frac{\partial \rho}{\partial y} \right)^2 - \frac{1}{(\gamma-1) \left(H_w - \frac{W^2}{2} \right)} \left[W_z \frac{\partial^2 W_z}{\partial y^2} + W_y \frac{\partial^2 W_y}{\partial y^2} + \left(\frac{\partial W_z}{\partial y} \right)^2 + \left(\frac{\partial W_y}{\partial y} \right)^2 \right] \tag{23}$$

Third and higher order y-derivatives, if required, can be obtained in a similar manner. The complete variation of any fluid property q

across the channel can then be expressed by a Taylor's series in $(y-y_m)$ from the various derivatives at the given streamline, such as the mean streamline

$$q(y) = q_m + (y-y_m)\left(\frac{\partial q}{\partial y}\right)_m + \frac{(y-y_m)^2}{2!}\left(\frac{\partial^2 q}{\partial y^2}\right)_m + \frac{(y-y_m)^3}{3!}\left(\frac{\partial^3 q}{\partial y^3}\right)_m + \frac{(y-y_m)^4}{4!}\left(\frac{\partial^4 q}{\partial y^4}\right)_m + \cdots \quad (24)$$

2223

Determination of Blade Profile

The blade profile can be obtained by a consideration of mass flow. At the chosen stations, mass flow across a constant z line from y_m to y is computed as a function of y according to the following equation:

$$M = \int_{y_m}^{y} \rho W_z \, dy \quad (25)$$

The variations of mass flow M and the magnitude of resultant velocity W at each station are plotted against y (fig. 2). Because the condition on the suction surface is more critical than that on the pressure surface, the blade shape on the suction side is determined first. From the plot of mass flow against y, a number of y_s's are chosen for a number of mass flows in the neighborhood of one-half the inlet mass flow, thus obtaining a number of suction surfaces. The corresponding velocities on the suction surfaces are read from the velocity plots (fig. 2). The one with the best velocity distribution is then chosen. After the suction surface is selected, the pressure surface and its velocity are determined in a similar manner by the total mass-flow requirement. If the shape or thickness of the blade or the velocity distribution on the blade obtained is not quite the one desired, the shape of and the flow on the mean streamline can be modified accordingly and the process repeated. Because each case takes a relatively small amount of computation, this modification is practical. Systematic building up of families of blades for various applications is also not difficult.

The accuracy of the blade coordinates obtained depends mainly on the accuracy of series representation and the accuracy to which the partial derivations are evaluated. For high-solidity blades, such as those investigated in reference 13, the first three terms in the series

will give sufficient accuracy. For low-solidity blades, more terms may be required. It may be noted that accurate representation of the flow variation by the series is difficult to achieve in the neighborhood very close to the leading and trailing edges; but from a practical point of view it is satisfactory to fair in the nose and the tail according to some standard shape after the blade coordinates are obtained up to a short distance away from these regions.

2223

The application of this design method will be greatly aided by the availability of detailed flow variations in typical bladings such as those given in references 13 and 16. If a typical solution of the type of blading to be designed is not available, either a direct problem may be solved first, or even better, the accuracy of the inverse solution can be ascertained in the manner described in the following section.

Method of Checking Solution

The inverse solution obtained by this method can be very conveniently checked and improved, if necessary, by the relaxation method utilizing the fluid state obtained in the solution. Inasmuch as the velocities are available in the solution, the equation for irrotational absolute flow (equation (A9) of reference 13) is now written as

$$\frac{\partial^2\psi}{\partial z^2} + \frac{\partial^2\psi}{\partial y^2} + \left(W_y \frac{\partial\rho}{\partial z} - W_z \frac{\partial\rho}{\partial y}\right) = 0 \tag{26}$$

The finite-difference form of equation (26) is then

$$\sum_{j=0}^{n} {}^{2}_{n}B^{i}_{j}\,\psi^{i} + \sum_{k=0}^{n} {}^{2}_{n}B^{i}_{k}\,\psi^{k} + \left[(W_y)^{i} \sum_{j=0}^{n} {}^{1}_{n}B^{i}_{j}\,\rho^{j} - (W_z)^{i} \sum_{k=0}^{n} {}^{1}_{n}B^{i}_{k}\,\rho^{k}\right] = 0 \tag{27}$$

where the same notation used in reference 13 is employed. A grid system is obtained by retaining the same z-stations used in the inverse solution and dividing the pitch distance into an appropriate number of divisions. The values of ψ, W, and ρ are most conveniently obtained by reading off the plots of integrated mass flow M, W, and ρ at each of the z-stations. The differentiation coefficients B's for equally spaced grid points as given in reference 17 can be applied throughout the domain for the present purpose by using the function values which are inside the blade but at equal spacing from the points in the channel (the first and last rows in tables III and IV). If the residuals obtained according to equation (27) require negligible change in ψ, the solution is entirely satisfactory. If the residuals are large enough to necessitate one cycle of relaxation, the net effect

may be a slight change in the specified mean streamline flow and in the velocity distribution on the resultant blade. If the residuals are so large as to warrant a few cycles of relaxation, the flow variation for this type of blading is established, which makes the design of other similar bladings very simple. In general, for problems in which some knowledge of the flow is available, no relaxation should be necessary except, perhaps, near the nose and tail when accurate detailed velocity distribution in these regions is desired.

2223

Special Case of Incompressible Flow

When the density is constant, the channel width ratio $P/(P-t)$ has a relation to $W_{z,m}$ similar to the relation it has to $(\rho W_z)_m$ in the compressible case (reference 13). A number of values of W_z are therefore prescribed at a number of chosen stations along the mean streamline to lead to a desirable thickness distribution of the blade. The solution of the incompressible problem continues in generally the same manner as it did for the compressible case with considerable simplification in the series terms and the integration process. In the incompressible case, of course, equations (12), (15), and (23) relating ρ and the velocities are unnecessary.

The first- and second-order derivatives expressed by equations (13), (14), (21), and (22) for the compressible case are simplified to:

$$\frac{\partial W_y}{\partial y} = \left(\tan \beta \frac{dW_y}{dz} - \frac{dW_z}{dz} \right) \cos^2 \beta \tag{28}$$

$$\frac{\partial W_z}{\partial y} = \left(\frac{dW_y}{dz} + \tan \beta \frac{dW_z}{dz} \right) \cos^2 \beta \tag{29}$$

$$\frac{\partial^2 W_y}{\partial y^2} = \left[\tan \beta \frac{d}{dz}\left(\frac{\partial W_y}{\partial y} \right) - \frac{d}{dz}\left(\frac{\partial W_z}{\partial y} \right) \right] \cos^2 \beta \tag{30}$$

and

$$\frac{\partial^2 W_z}{\partial y^2} = \frac{d}{dz}\left(\frac{\partial W_y}{\partial y} \right) - \tan \beta \left(\frac{\partial^2 W_y}{\partial y^2} \right) \tag{31}$$

for the incompressible case. The equation for obtaining mass flow becomes $M = \rho \int_{y_m}^{y} W_z \, dy$.

Illustrative Examples

The procedure outlined in the preceding sections has been applied to the design of several highly cambered thick turbine blades for either compressible or incompressible flow.

First and second examples. - In the first example, the shape of the mean streamline and the variation of axial velocity obtained in the incompressible solution of the blade given in reference 13 are taken as the specified values in order to determine whether the original blade will be reproduced. The shape of the mean streamline is shown in figure 1 and the thickness distribution of the blade is shown in figure 3. As a further check of the method, the z-stations chosen in this calculation correspond to every other z-station used in reference 13, so that the velocities obtained along these stations can also be compared with the solutions obtained in reference 13. The given quantities were inlet angle β_i, $41^\circ\ 18'$; exit angle β_e, $-52^\circ\ 57'$; axial chord L, 1.5 inches; and pitch P, 1.017 inches.

2223

The same data are used in the second example in which a compressible solution for an inlet Mach number of 0.42 is obtained. The axial-velocity variation on the mean streamline used in the first example is now taken as the specific-mass-flow variation on the mean streamline. This example is presented mainly to illustrate the difference in incompressible and compressible solutions for the same mean streamline shape and the same ratio of specific mass flow.

The complete computation for the flow on the mean streamline and the determination of the first- and second-order derivatives of W_z, W_y, and ρ in the pitch direction at the mean streamline for these two cases is given in tables I and II. Only three terms in the series are used because the direct solutions given in reference 13 indicate that they will be sufficient for engineering accuracy. The central-point fourth-degree differentiation formula is used at the regular stations z_3 to z_{16}. Because the first and last stations inside the channel employed in reference 13 are not close enough to the leading and trailing edges, respectively, two extra points are computed at stations 6.75 and 12.25 by the use of the unequal interval differentiation formula given in reference 18. These two points are so designated because they are located at a distance of a quarter of the regular spacing away from stations 7 and 12, respectively. This combination is unnecessary for other cases.

The velocities and the densities used in the calculation are nondimensionalized as follows:

$$W_z^* = \frac{W_z}{W_{z,i}}$$

$$W_y^* = \frac{W_y}{W_{z,i}}$$

$$\rho^* = \frac{\rho}{\rho_i}$$

2223

The mass flow M^*, being divided by $\rho_i W_{z,i}$, has the dimension of length:

$$M^* = \frac{M}{\rho_i W_{z,i}}$$

For the compressible case, the ratio of H_w to $W_{z,i}^2$ is equal to 25.78, which is the value used in the construction of the two density graphs involved in the calculation, the reduced versions of which are shown in figures 4 and 5.

The values in columns 2, 5, 8, 9, 12, and 13 of table I and 7, 8, 13, 14, 22, and 23 of table II are used to compute the variation of W_z and W_y in the pitch direction by the power series. The calculation of density follows directly as does the integration across the channel for mass flow, the mass flow being determined numerically. Because the specific mass flow ρW_z was made dimensionless with its inlet value, the numerical value for the mass flow is equal to the pitch, the height being considered unity. This indicates that the integration for mass flow along the pitch direction starting at the mean streamline was considered to be complete in either the plus or minus direction when a value equal to one-half the pitch distance or one-half the total mass flow was reached. Thus the channel flow and the blade coordinates were obtained. This calculation at one station, 10, is shown in tables III and IV for the two cases, respectively.

The blade profile obtained by interpolating y_s and y_p for one-half of the inlet mass-flow value is shown in figure 6. Because of the same mean streamline shape and the same variation of specific mass flow on the mean streamline prescribed in the incompressible and compressible cases, the blades obtained for these two cases look quite similar except that the compressible one is somewhat thicker and the suction surface of the compressible solution is situated farther from the given mean streamline; these results are consistent with the direct solutions given in reference 13. The velocities obtained in the two cases (fig. 7), however, are quite different. Those in the compressible

solution are, in general, higher than those in the incompressible case, principally because of the high velocity on the mean streamline resulting from the use of the same $(\rho W_z)_m$ and a decreasing ρ along the mean streamline in the compressible case.

The blade coordinates obtained in the incompressible solution are compared with those of the original blade in figure 8. The velocities at the six regular stations in the channel are compared (figs. 9 to 11) with the values obtained in the relaxation solution of the original blade reported in reference 13. These four figures show that, in general, the present solution is satisfactory. The relatively large differences near the leading and trailing edges are partly due to the inaccuracy in the second-degree polynomial approximation in the present calculation and partly due to the inaccuracy of the numerical solution obtained in reference 13 caused by the relatively coarse grid used in these regions.

2223

As a check of the consistency of the solution, an integration of the velocity along the blade profile obtained in the same example was made and compared with the circulation value computed from the inlet and exit tangential velocities and the pitch. The two are in agreement within 1 percent.

Third and fourth examples. - In the previous two examples, the mean streamlines and specific-mass-flow distributions prescribed were not entirely arbitrary, having been obtained from the results of a direct problem for incompressible flow. The possibility of obtaining an unrealistic blade shape was, for this reason, largely eliminated. Consequently, in order to give the method a still more rigorous test, the thickness distribution (fig. 12) and mean blade line (fig. 13) for the hub section of an experimental cooled turbine blade were arbitrarily chosen from which a mean streamline and specific mass flow were estimated by means discussed in the section "General Description of Method."

In addition to the mean blade line and thickness distribution, the following data were used: inlet Mach number, 0.42; inlet angle, 36.2°; exit angle, 42.7°; axial chord, 1.8 inches; and pitch, 1.176 inches. The mean blade line was faired into the inlet and exit directions (fig. 14) with modification to obtain a mean streamline according to the information obtained for a typical turbine blade in reference 13 (see fig. 8). The thickness distribution was used to obtain the specific-mass-flow distribution along the mean streamline (dashed curve in fig. 15) according to results obtained in reference 13. After the flow on the mean streamline was calculated, it was then extended out from the mean streamline across the channel by means of power series as before.

Both compressible and incompressible solutions were completed, the incompressible case being considered first because of its relative

simplicity. The results of the incompressible case served as a guide to obtaining better prescribed values for the compressible case. The blade obtained in the incompressible solution has a slightly higher thickness distribution than was wanted and, because results obtained in the first two examples indicate that the compressible blade will be thicker than the incompressible for the same specific-mass-flow distribution, this distribution was depressed by a linear proportioning (fig. 15) in order to obtain better starting values for the compressible case and consequently a thinner blade (fig. 14). The same mean streamline numerically smoothed to give small fourth differences was used in both cases.

2223

As a check of the accuracy of the last solution, a grid having the same spacing in the z-direction used in the inverse solution (0.18) and a grid spacing of 0.147 in the y-direction is chosen, and the residuals at the grid points are computed according to equation (27) using the central point second-degree differentiation formula. As shown in table V, the residuals are rather small when they are compared with the magnitude of the coefficient at the points (-154.3). As an indication of the percentage error in the velocity, these residuals are first divided by -154.3, resulting in an approximate change in the ψ value at each point. Then the probable error in $\partial\psi/\partial y$ or ρW_z is calculated. The result is shown in table VI, which indicates that the solution obtained is sufficiently accurate for ordinary purposes.

DESIGNING BLADES FOR COMPRESSIBLE FLOW ALONG ARBITRARY STREAM FILAMENT OF REVOLUTION

Basic Relations

The blade design method presented in the section "Designing Blades for Compressible Flow in Plane or on Cylindrical Surface" can be very easily extended to the more general case of flow along an arbitrary stream filament of revolution having a varying normal thickness (fig. 16). When only an average value in the stream filament of revolution, as represented by the flow on the mean stream surface of revolution described by a set of orthogonal coordinates l and φ (fig. 16), is considered, the equation of continuity for steady relative flow and the equation of irrotational absolute flow are given in reference 13 as follows:

$$\frac{\partial(\tau\rho W_l r)}{\partial l} + \frac{\partial(\tau\rho W_\varphi)}{\partial\varphi} = 0 \qquad (1')$$

$$\frac{\partial W_\varphi}{\partial l} - \frac{1}{r}\frac{\partial W_l}{\partial\varphi} + \frac{W_\varphi \sin\sigma}{r} + 2\omega\sin\sigma = 0 \qquad (2')$$

where primes in equation numbers indicate equations similar to those of the cylindrical case.

When the fluid flow along a streamline $S(l,\varphi) = 0$ on the mean surface of revolution is considered, it is convenient to write any quantity q on S as a function of l only. Then the total derivative of q with respect to l, following the streamline, is

$$\frac{dq}{dl} = \frac{\partial q}{\partial l} + \frac{\partial q}{\partial \varphi}\frac{d\varphi}{dl} = \frac{\partial q}{\partial l} + \frac{\partial q}{\partial \varphi}\frac{1}{r}\frac{W_\varphi}{W_l} = \frac{\partial q}{\partial l} + \frac{\tan \beta}{r}\frac{\partial q}{\partial \varphi} \tag{9'}$$

2223

when

$$\tan \beta = \frac{W_\varphi}{W_l} = r\frac{d\varphi}{dl}$$

When the preceding relation is used, the continuity and irrotationality conditions can be written as

$$\frac{d(\tau \rho W_l r)}{dl} - \tan \beta \frac{\partial(\tau \rho W_l)}{\partial \varphi} + \frac{\partial(\tau \rho W_\varphi)}{\partial \varphi} = 0 \tag{10'}$$

and

$$\frac{dW_\varphi}{dl} - \frac{1}{r}\frac{\partial W_l}{\partial \varphi} - \frac{\tan \beta}{r}\frac{\partial W_\varphi}{\partial \varphi} + \left(\frac{W_\varphi}{r} + 2\omega\right) \sin \sigma = 0 \tag{11'}$$

The variation of density throughout the flow region, in general, is obtained from the velocity by using the following equation:

$$\rho^* = \frac{\rho}{\rho_i} = \left(\frac{I + \frac{1}{2}\omega^2 r^2 - \frac{1}{2}W^2}{h_i}\right)^{\frac{1}{\gamma - 1}} \tag{12'}$$

In order to obtain the density on the starting (mean) streamline, equation (12') is written in the following form (compare with equation (7a) of reference 13):

$$\Sigma = \left(1 - \frac{\Phi}{\Sigma}\right)^{\frac{2}{\gamma - 1}} \tag{12a'}$$

where

$$\Sigma = \rho^{*2}\left(\frac{I + \frac{1}{2}\omega^2 r^2}{h_i}\right)^{-\frac{2}{\gamma-1}}$$

and

$$\Phi = (\rho^* W_l^* \sec\beta)^2 \left(\frac{W_{l,i}^2}{2\,h_i}\right)\left(\frac{I + \frac{1}{2}\omega^2 r^2}{h_i}\right)^{-\frac{\gamma+1}{\gamma-1}}$$

2223

Once the general relation between Σ and Φ is available, the evaluation of ρ^* for certain given values of $\rho^* W_l^* \sec\beta$ along the chosen (mean) streamline is made simple if auxiliary tables or graphs giving $\left(\frac{I + \frac{1}{2}\omega^2 r^2}{h_i}\right)^{-\frac{2}{\gamma-1}}$ and $\left(\frac{W_{l,i}^2}{2\,h_i}\right)\left(\frac{I + \frac{1}{2}\omega^2 r^2}{h_i}\right)^{-\frac{\gamma+1}{\gamma-1}}$ as functions of r are first obtained.

The determination of the flow along the starting (mean) streamline (fig. 17) proceeds very much the same as in the case of plane flow or flow on a cylindrical surface. The shape of the streamline gives $\sec\beta$. The variation of $\rho^* W_l^*$ is obtained from the blade-thickness variation along the mean surface of revolution as follows: If the value of ρW_l on the mean streamline represents its average value in the circumferential direction

$$\tau(\rho W_l)_m\,(P-t) = (\tau \rho W_l P)_i \tag{32}$$

But

$$\frac{P_i}{P} = \frac{r_i}{r} \tag{33}$$

hence

$$\frac{\tau(\rho W_l)_m\, r}{(\tau \rho W_l r)_i} = \frac{P}{P-t} \tag{34}$$

Although there is always some deviation from this simple relation, especially around the leading and trailing edges, a relation between the two terms in equation (34) similar to that between $(\rho^* W_z^*)_m$ and

$P/(P-t)$ in the previous cylindrical case can be expected. Then, from $\tau^*(\rho^* W_l^*)_m r^*$, $(\rho^* W_l^*)_m$ is calculated and combined with $\sec \beta$ from which ρ_m^* is obtained by equation (12a'). After ρ_m^* is determined, $W_{l,m}^*$ and then $W_{\varphi,m}^*$ are easily calculated.

Variation of Fluid State in Pitch Direction

The first-order partial derivatives of W_l, W_φ, and ρ with respect to φ are readily obtained from equations (10'), (11'), and (12') as:

$$\frac{\partial W_l}{\partial \varphi} = \left[r \frac{dW_\varphi}{dl} + \frac{\tan \beta}{\tau \rho} \frac{d(\tau \rho W_l r)}{dl} + (W_\varphi + 2\omega r) \sin \sigma \right] \cos^2 \beta \qquad (13')$$

$$\frac{\partial W_\varphi}{\partial \varphi} = \left\{ \tan \beta \left[r \frac{dW_\varphi}{dl} + (W_\varphi + 2\omega r) \sin \sigma \right] - \frac{1}{\tau \rho} \frac{d(\tau \rho W_l r)}{dl} \right\} \cos^2 \beta \qquad (14')$$

$$\frac{1}{\rho} \frac{\partial \rho}{\partial \varphi} = - \frac{1}{(\gamma - 1)\left(I + \frac{1}{2} \omega^2 r^2 - \frac{1}{2} W^2 \right)} \left(W_l \frac{\partial W_l}{\partial \varphi} + W_\varphi \frac{\partial W_\varphi}{\partial \varphi} \right) \qquad (15')$$

In a manner similar to that of the case of plane or cylindrical flow the second-order partial derivatives of W_l, W_φ, and ρ are obtained as follows:

$$\frac{\partial^2 W_\varphi}{\partial \varphi^2} = \left\{ \frac{2}{\tau \rho^2} \frac{\partial \rho}{\partial \varphi} \frac{d(\tau \rho W_l r)}{dl} - \frac{1}{\tau \rho} \frac{d}{dl} \left[\tau r \left(\rho \frac{\partial W_l}{\partial \varphi} + W_l \frac{\partial \rho}{\partial \varphi} \right) \right] + \tan \beta \left(r \frac{d}{dl} \frac{\partial W_\varphi}{\partial \varphi} + \sin \sigma \frac{\partial W_\varphi}{\partial \varphi} \right) \right\} \cos^2 \beta \qquad (21')$$

$$\frac{\partial^2 W_l}{\partial \varphi^2} = r \frac{d}{dl} \frac{\partial W_\varphi}{\partial \varphi} - \tan \beta \frac{\partial^2 W_\varphi}{\partial \varphi^2} + \sin \sigma \frac{\partial W_\varphi}{\partial \varphi} \qquad (22')$$

$$\frac{1}{\rho} \frac{\partial^2 \rho}{\partial \varphi^2} = \frac{2 - \gamma}{\rho^2} \left(\frac{\partial \rho}{\partial \varphi} \right)^2 - \frac{1}{(\gamma - 1)\left(I + \frac{1}{2} \omega^2 r^2 - \frac{1}{2} W^2 \right)} \left[W_l \frac{\partial^2 W_l}{\partial \varphi^2} + W_\varphi \frac{\partial^2 W_\varphi}{\partial \varphi^2} + \left(\frac{\partial W_l}{\partial \varphi} \right)^2 + \left(\frac{\partial W_\varphi}{\partial \varphi} \right)^2 \right] \qquad (23')$$

2223

After the variation of fluid state in the circumferential direction is determined, the mass flow across a constant l line from φ_m to φ is computed by

$$M = r\tau \int_{\varphi_m}^{\varphi} \rho W_l \, d\varphi \tag{25'}$$

from which the blade coordinates are determined as in the previous case. If checking is desired, the following equations are to be used:

$$\frac{\partial^2 \psi}{\partial l^2} + \left(\frac{\sin \sigma}{r} - \frac{\partial \ln \tau}{\partial l} \right) \frac{\partial \psi}{\partial l} + \frac{1}{r^2} \frac{\partial^2 \psi}{\partial \varphi^2} + \tau \left(W_\varphi \frac{\partial \rho}{\partial l} - \frac{W_l}{r} \frac{\partial \rho}{\partial \varphi} + 2\omega\rho \sin \sigma \right) = 0 \tag{26'}$$

$$\sum_{j=0}^{n} \left[{}_{n}^{2}B_{j}^{i} + \left(\frac{\sin \sigma}{r} - \frac{\partial \ln \tau}{\partial l} \right)^{i} {}_{n}^{1}B_{j}^{i} \right] \psi^j + \sum_{k=0}^{n} \frac{{}_{n}^{2}B_{k}^{i}}{(r^i)^2} \psi^k + \tau^i \left[W_\varphi{}^i \sum_{j=0}^{n} {}_{n}^{1}B_{j}^{i} \rho^j - \left(\frac{W_l}{r} \right)^i \sum_{k=0}^{n} {}_{n}^{1}B_{k}^{i} \rho^k + 2\omega(\rho \sin \sigma)^i \right] = 0 \tag{27'}$$

where the same notation used in reference 13 is employed.

SUMMARY OF RESULTS

A rapid method for designing turbomachine blades of a given turning and a desirable blade-thickness distribution for a compressible nonviscous fluid flow along an arbitrary stream filament of revolution is presented. The method utilizes the guiding effects of the blade shape on the mean streamline shape and of the blade thickness on the specific mass flow along the mean streamline. After the flow on the mean streamline is determined, the extension of the solution from the mean streamline to the blade surfaces is accomplished by the use of a power series. A number of blade profiles are obtainable for the total mass-flow requirement, and one is chosen for the best velocity distribution on the blade. The results obtained in the solution can be used for a direct check on the accuracy of series approximation and, also, for the more accurate determination of the velocity distribution along the leading and trailing edges of the blade.

2223

2223

The method is illustrated with the design of several cascades of airfoils. In each case either some indication of the accuracy of the solution is given or the relation between the incompressible and compressible problems are shown. In the first case, the results obtained in an incompressible direct solution were used as prescribed values for the inverse problem to show that the original blade can be relatively easily reproduced with adequate accuracy. The variation of the velocity and its components across the channel was shown to compare favorably with those obtained in the direct solution and an integration around the blade for the circulation checked with that obtained from inlet and exit values within 1 percent. In the second problem, the same mean streamline and specific-mass-flow distribution along it were used; but this time the density was allowed to vary as in compressible flow and a comparison was made between the blades obtained in the first two cases. In the third and last problem, an arbitrary mean streamline and specific-mass-flow distribution were chosen, the blade obtained, and the solution checked by calculation of the residuals as in a direct relaxation solution. Because the residuals were small the solution was considered to be reasonably accurate. A computation designed to give some indication of the accuracy of the velocities by dividing the derivative of the error in the stream function ψ by the derivative of ψ itself showed them to be accurate generally within 1 percent except near the blade boundaries where an end-point formula was necessarily used to obtain derivatives.

Because the surface of revolution, on which the blades are located, is completely arbitrary, the method can be applied to axial-flow, radial-flow, and mixed-flow turbomachines. The variation in the normal distance between the stream surfaces of revolution can be taken into account, thus incorporating into the design the principal effect of three-dimensional flow. The method is readily applied to the design of channels on a plane and on a general surface of revolution.

Lewis Flight Propulsion Laboratory,
National Advisory Committee for Aeronautics,
Cleveland, Ohio, May 31, 1951.

REFERENCES

1. Weinig, F.: Die Strömung um die Schaufeln von Turbomaschinen. Johann Ambrosius Barth (Leipzig), 1935.

2. Ackeret, J.: The Design of Closely Spaced Blade Grids. Schweiz. Bauzeitung, vol. 120, no. 9, Aug. 29, 1942, pp. 103-108.

3. Mutterperl, William: A Solution of the Direct and Inverse Potential Problems for Arbitrary Cascades of Airfoils. NACA ARR L4K22b, 1944.

4. Lighthill, M. J.: A Mathematical Method of Cascade Design. R. & M. No. 2104, British A.R.C., June 1945.

5. Diesendruck, Leo: Iterative Interference Methods in the Design of Thin Cascade Blades. NACA TN 1254, 1947.

6. Goldstein, Arthur W., and Jerison, Meyer: Isolated and Cascade Airfoils with Prescribed Velocity Distribution. NACA Rep. 869, 1947. (Formerly NACA TN 1308.)

7. Hansen, Arthur G., and Yohner, Peggy L.: A Numerical Procedure for Designing Cascade Blades with Prescribed Velocity Distributions in Incompressible Potential Flow. NACA TN 2101, 1950.

8. Spurr, Robert A., and Allen, H. Julian: A Theory of Unstaggered Airfoil Cascades in Compressible Flow. NACA Rep. 888, 1947. (Formerly NACA RM A7E29, 1947.)

9. Alpert, Sumner: Design Method for Two-Dimensional Channels for Compressible Flow with Application to High-Solidity Cascades. NACA TN 1931, 1949.

10. Lin, C. C.: On the Subsonic Flow through Circular and Straight Lattices of Airfoils. Jour. Math. and Phys., vol. XXXVIII, no. 2, July 1949, pp. 117-130.

11. Costello, George R.: Methods of Designing Cascade Blades with Prescribed Velocity Distributions in Compressible Potential Flows. NACA TN 1970, 1949.

12. Betz, A., and Flügge-Lotz, I.: Design of Centrifugal Impeller Blades. NACA TM 902, 1939.

13. Wu, Chung-Hua, and Brown, Curtis A.: Method of Analysis for Compressible Flow Past Arbitrary Turbomachine Blades on General Surface of Revolution. NACA TN 2407, 1951.

2223

14. Dreyfus, L. A.: A Three-dimensional Theory of Turbine Flow and its Application to the Design of Wheel Vanes for Francis and Propeller Turbines. ACTA Polytechnica, Mech. Eng. Series, vol. 1, nr. 1 (Stockholm), 1947.

15. Reissner, Hans: Blade Systems of Circular Arrangement in Steady, Compressible Flow. Studies and Essays. Courant Anniversary Volume, Interscience Publishers, Inc., (New York), 1948, pp. 307-327.

16. Stanitz, John D., and Ellis, Gaylord O.: Two-Dimensional Compressible Flow in Centrifugal Compressors with Straight Blades. NACA Rep. 954, 1950. (Formerly NACA TN 1932.)

17. Bickley, W. G.: Formulae for Numerical Differentiation. The Math. Gazette, vol. XXV, no. 263, Feb. 1941, pp. 19-27.

18. Wu, Chung-Hua: Formulas and Tables of Coefficients for Numerical Differentiation with Function Values Given at Unequally Spaced Points and Application to Solution of Partial Differential Equations. NACA TN 2214, 1950.

2223

TABLE I - COMPUTATION OF FLOW ON MEAN STREAMLINE AND FIRST- AND SECOND-ORDER y-DERIVATIVES AT THE MEAN STREAMLINE OF FIRST EXAMPLE
(INCOMPRESSIBLE FLOW)

		①	②	③	④	⑤	⑥	⑦	⑧	⑨	⑩	⑪	⑫	⑬
Station	z	y_m	$W^*_{z,m}$	$\tan \beta_m$ $\frac{d①}{dz}$	$\sec^2 \beta_m$ $③^2 + 1$	$W^*_{y,m}$ ②③	$\frac{d\,W^*_{z,m}}{dz}$ $\frac{d②}{dz}$	$\frac{d\,W^*_{y,m}}{dz}$ $\frac{d⑤}{dz}$	$\left(\frac{\partial W^*_z}{\partial y}\right)_m$ $\frac{③⑥+⑦}{④}$	$\left(\frac{\partial W^*_y}{\partial y}\right)_m$ $\frac{③⑦-⑥}{④}$	$\frac{d}{dz}\left(\frac{\partial W^*_z}{\partial y}\right)_m$ $\frac{d⑧}{dz}$	$\frac{d}{dz}\left(\frac{\partial W^*_y}{\partial y}\right)_m$ $\frac{d⑨}{dz}$	$\left(\frac{\partial^2 W^*_y}{\partial y^2}\right)_m$ $\frac{③⑪-⑩}{④}$	$\left(\frac{\partial^2 W^*_z}{\partial y^2}\right)_m$ ⑪-③⑫
1	-1.4084	-0.3728	1.0000	--------	-------	--------	--------	--------	--------	--------	--------	--------	--------	--------
2	-1.1541	- .1494	1.0000	--------	-------	--------	--------	--------	--------	--------	--------	--------	--------	--------
3	- .8999	.0740	1.0000	0.89108	1.79402	.89108	--------	--------	--------	--------	--------	--------	--------	--------
4	- .6456	.3060	.9990	.93556	1.87527	.93462	--------	--------	--------	--------	--------	--------	--------	--------
5	- .3914	.5517	.9771	1.03618	2.07367	1.01245	.25467	.40963	0.32479	0.08187	--------	--------	--------	--------
6	- .1371	.8178	1.1500	.93615	1.87638	1.07657	1.01252	- .39092	.29682	- .73465	--------	--------	--------	--------
6.75	.0535	.9684	1.3659	.65622	1.43062	.89633	1.08548	-1.67726	- .67450	-1.52810	-5.42823	0.65833	4.09629	-2.02974
7	.1171	1.0070	1.4310	.54290	1.29474	.77689	.83681	-1.76538	-1.01262	-1.38656	-5.49465	.43023	4.42423	-1.97168
8	.3714	1.0922	1.5410	.15759	1.02483	.24285	.20256	-2.15563	-2.07225	- .52913	-1.74154	4.16951	2.34050	3.80067
9	.6256	1.0905	1.5520	- .17470	1.03052	- .27113	- .08784	-1.93581	-1.86359	.41341	2.12073	3.07270	-2.57882	2.62218
10	.8799	1.0050	1.5000	- .48718	1.23734	- .73077	- .36054	-1.65736	-1.19750	.94394	2.91580	1.20754	-2.83195	- .17213
11	1.1341	.8424	1.3710	- .80665	1.65068	-1.10592	- .63199	-1.31032	- .48497	1.02319	2.60927	- .55502	-1.30950	-1.61133
12	1.3884	.5938	1.1930	-1.15578	2.33583	-1.37885	- .73497	- .70788	.06061	.66491	1.48324	-2.66657	.68444	-1.87551
12.25	1.4519	.5170	1.1430	-1.24560	2.55152	-1.42372	- .76104	- .57670	.14550	.57980	1.12891	-1.97290	.52068	-1.32434
13	1.6426	.2620	1.0242	-1.42353	3.02644	-1.45798	- .46772	.06181	.24042	- .12547	--------	--------	--------	--------
14	1.8969	- .1119	.9680	-1.43337	3.05455	-1.38750	- .00544	.23739	.08027	- .10962	--------	--------	--------	--------
15	2.1511	- .4600	.9980	-1.36644	2.86716	-1.36371	--------	--------	--------	--------	--------	--------	--------	--------
16	2.4054	- .8090	1.0000	-1.34897	2.81972	-1.34897	--------	--------	--------	--------	--------	--------	--------	--------
17	2.6596	-1.1458	1.0000	--------	-------	--------	--------	--------	--------	--------	--------	--------	--------	--------
18	2.9139	-1.4826	1.0000	--------	-------	--------	--------	--------	--------	--------	--------	--------	--------	--------

TABLE II - COMPUTATION OF FLOW ON MEAN STREAMLINE AND FIRST- AND SECOND-ORDER

Station	z	① y_m	② $(\rho^* W_z^*)_m$	③ $\tan \beta_m$ $\frac{d①}{dz}$	④ $\sec^2 \beta_m$ $③^2 + 1$	⑤ $(\rho^* W_z^* \sec \beta)_m^2$ $②^2$ ④	⑥ ρ_m^* From ⑤ and fig. 4	⑦ $W_{z,m}^*$ $\frac{②}{⑥}$	⑧ $W_{y,m}^*$ ③⑦	⑨ $\frac{d W_{y,m}^*}{dz}$ $\frac{d⑧}{dz}$	⑩ $\frac{d (\rho^* W_z^*)_m}{dz}$ $\frac{d②}{dz}$	⑪ $\frac{1}{\rho_m^*}$ $\frac{1}{⑥}$	⑫ $\frac{1}{\rho_m^*} \frac{d (\rho^* W_z^*)_m}{dz}$ ⑩ ⑪
1	-1.4084	-0.3728	1.0000	--------	-------	-----	------	-------	--------	--------	--------	-------	--------
2	-1.1541	- .1494	1.0000	--------	-------	-----	------	-------	--------	--------	--------	-------	--------
3	- .8999	.0740	1.0000	0.89108	1.79402	1.794	0.9989	1.00110	0.89206	--------	--------	-------	--------
4	- .6456	.3060	.9990	.93556	1.87527	1.872	.9942	1.00483	.94008	--------	--------	-------	--------
5	- .3914	.5517	.9771	1.03618	2.07367	1.980	.9875	.98947	1.02527	0.51913	.25467	1.01266	0.25789
6	- .1371	.8178	1.1500	.93615	1.87638	2.482	.9528	1.20697	1.12990	- .29567	1.01252	1.04954	1.06268
6.75	.0535	.9684	1.3659	.65622	1.43062	2.669	.9381	1.45603	.95548	-1.78473	1.08548	1.06598	1.15710
7	.1171	1.0070	1.4310	.54290	1.29474	2.651	.9397	1.52283	.82674	-1.86758	.83681	1.06417	.89051
8	.3714	1.0922	1.5410	.15759	1.02483	2.434	.9564	1.61125	.25392	-2.28571	.20256	1.04559	.21179
9	.6256	1.0905	1.5520	- .17470	1.03052	2.482	.9528	1.62888	- .28457	-2.05532	- .08784	1.04954	- .09219
10	.8799	1.0050	1.5000	- .48718	1.23734	2.784	.9287	1.61516	- .78687	-1.87747	- .36054	1.07677	- .38822
11	1.1341	.8424	1.3710	- .80665	1.65068	3.103	.9000	1.52333	-1.22879	-1.61583	- .63199	1.11111	- .70221
12	1.3884	.5938	1.1930	-1.15578	2.33583	3.324	.8773	1.35985	-1.57169	- .82525	- .73497	1.13986	- .83776
12.25	1.4519	.5170	1.1430	-1.24560	2.55152	3.333	.8763	1.30435	-1.62470	- .63878	- .76104	1.14116	- .86847
13	1.6426	.2620	1.0242	-1.42353	3.02644	3.175	.8927	1.14731	-1.63323	.25782	- .46772	1.12020	- .52394
14	1.8969	- .1119	.9680	-1.43337	3.05455	2.862	.9222	1.04966	-1.50455	.36881	- .00544	1.08436	- .00590
15	2.1511	- .4600	.9980	-1.36644	2.86716	2.856	.9225	1.08184	-1.47827	--------	--------	-------	--------
16	2.4054	- .8090	1.0000	-1.34897	2.81972	2.820	.9257	1.08026	-1.45724	--------	--------	-------	--------
17	2.6596	-1.1458	1.0000	--------	-------	-----	------	-------	--------	--------	--------	-------	--------
18	2.9139	-1.4826	1.0000	--------	-------	-----	------	-------	--------	--------	--------	-------	--------

y-DERIVATIVES AT THE MEAN STREAMLINE OF SECOND EXAMPLE (COMPRESSIBLE FLOW)

(13) $\left(\frac{\partial w_z^*}{\partial y}\right)_m$ $\frac{(3)(12)+(9)}{(4)}$	(14) $\left(\frac{\partial w_y^*}{\partial y}\right)_m$ $\frac{(3)(9)-(12)}{(4)}$	(15) Portion of equation (15) $\frac{(7)(13)+(8)(14)}{(11)}$	(16) Portion of equation (15) $.2\left[(7)^2+(8)^2\right]-10.312$	(17) $\left(\frac{\partial \rho^*}{\partial y}\right)_m$ $\frac{(15)}{(16)}$	Portion of equation (21) (18) $(6)(13)+(7)(17)$	(19) $\frac{d(18)}{dz}$	(20) $\frac{d(14)}{dz}$	(21) $2(12)(17)-(19)$	(22) $\left(\frac{\partial^2 w_y^*}{\partial y^2}\right)_m$ $\frac{(11)(21)+(3)(20)}{(4)}$	(23) $\left(\frac{\partial^2 w_z^*}{\partial y^2}\right)_m$ $(20)-(3)(22)$
--------	--------	--------	--------	--------	--------	--------	--------	--------	--------	--------
--------	--------	--------	--------	--------	--------	--------	--------	--------	--------	--------
--------	--------	--------	--------	--------	--------	--------	--------	--------	--------	--------
--------	--------	--------	--------	--------	--------	--------	--------	--------	--------	--------
0.37921	0.13504	0.50725	-9.90595	-0.05121	0.32380	--------	--------	--------	--------	--------
.37261	- .71386	- .34002	-9.76531	.03482	.39705	--------	--------	--------	--------	--------
- .71676	-1.62746	-2.43778	-9.70541	.25118	- .30667	-4.34319	0.68130	4.92447	3.98182	-1.93165
-1.06903	-1.47089	-2.67250	-9.71150	.27519	- .58550	-4.48125	.30905	4.97137	4.21565	-1.97963
-2.19776	- .55814	-3.52228	-9.77988	.36016	-1.52163	-1.62207	4.42590	1.77463	2.49116	4.03332
-1.97882	.43789	-3.18986	-9.76515	.32666	-1.35333	1.78075	3.34414	-1.84098	-2.44188	2.91754
-1.36449	1.05297	-2.81622	-9.66642	.29134	- .79664	2.41248	1.60341	-2.63869	-2.92758	.17715
- .63573	1.21503	-2.21530	-9.54591	.23207	- .21864	2.05021	- .62334	-2.37613	-1.29481	-1.66780
.06123	.76699	- .98451	-9.44812	.10420	.19541	1.14733	-2.64875	-1.32192	.66553	-1.87954
.17362	.65221	- .73012	-9.44380	.07731	.25298	.78433	-2.17306	- .91861	.65000	-1.36342
.33163	.05185	.26406	-9.51525	.02775	.32788	--------	--------	--------	--------	--------
.12351	- .17114	.35701	-9.63891	- .03704	.07502	--------	--------	--------	--------	--------
--------	--------	--------	--------	--------	--------	--------	--------	--------	--------	--------
--------	--------	--------	--------	--------	--------	--------	--------	--------	--------	--------
--------	--------	--------	--------	--------	--------	--------	--------	--------	--------	--------
--------	--------	--------	--------	--------	--------	--------	--------	--------	--------	--------

TABLE III - COMPUTATION OF VELOCITY COMPONENTS AND MASS FLOW AT STATION 10 OF THE FIRST EXAMPLE (INCOMPRESSIBLE FLOW)

$[z_{10} = 0.8799;\ y_m = 1.0050;\ \Delta y_p = 0.13333;\ \Delta y_s = -0.09933]$

Station $n\Delta y$	① y $y_m + n(\Delta y)$	② $y - y_m$ $n\Delta y$	③ $\frac{(y-y_m)^2}{2}$ $\frac{n^2}{2}(\Delta y)^2$	④ $W_{z,m}^*$	⑤ $\left(\frac{\partial W_z^*}{\partial y}\right)_m$	⑥ $\left(\frac{\partial^2 W_z^*}{\partial y^2}\right)_m$	⑦ W_z^* ④+②⑤+③⑥	⑧ $W_{y,m}^*$	⑨ $\left(\frac{\partial W_y^*}{\partial y}\right)_m$	⑩ $\left(\frac{\partial^2 W_y^*}{\partial y^2}\right)_m$	⑪ W_y^* ⑧+②⑨+③⑩	⑫ W^* $\sqrt{⑦^2 + ⑪^2}$	⑬ M^* $\int_{y_m}^{y} ⑦\,dy$	⑭ Blade y coordinate obtained for $M^* = \pm 0.5085$
$4\Delta y_p$	1.5383	0.53333	0.14222	------	-------	--------	0.83686	--------	-------	--------	-0.63010	1.04755	0.62534	-------
$3\Delta y_p$	1.4050	.40000	.08000	------	-------	--------	1.00723	--------	-------	--------	- .57975	1.16216	.50236	1.41120
$2\Delta y_p$	1.2717	.26667	.03556	------	-------	--------	1.17454	--------	-------	--------	- .57975	1.30983	.35688	-------
Δy_p	1.1383	.13333	.00889	------	-------	--------	1.33881	--------	-------	--------	- .63009	1.47967	-------	-------
y_m	1.0050	--------	-------	1.5000	-1.19750	-0.17213	1.50000	-0.73077	0.94394	-2.83195	- .73077	1.66854	-------	-------
Δy_s	.9057	- .09933	.00493	------	-------	--------	1.61810	--------	-------	--------	- .83849	1.82236	-------	-------
$2\Delta y_s$	.8063	- .19867	.01973	------	-------	--------	1.73451	--------	-------	--------	- .97418	1.98936	-.32141	-------
$3\Delta y_s$	.7070	- .29800	.04440	------	-------	--------	1.84921	--------	-------	--------	-1.13780	2.17121	-.49941	.70208
$4\Delta y_s$	.6077	- .39733	.07894	------	-------	--------	1.96221	--------	-------	--------	-1.32938	2.37013	-.68873	-------

NACA

TABLE IV - COMPUTATION OF VELOCITY COMPONENTS AND MASS FLOW AT STATION 10 OF THE SECOND EXAMPLE (COMPRESSIBLE FLOW)

$\left[z_{10} = 0.8799;\ y_m = 1.0050;\ \Delta y_p = 0.13333;\ \Delta y_s = -0.09933\right]$

Station $n\Delta y$	① y $y_m + n(\Delta y)$	② $y - y_m$ $n\Delta y$	③ $\frac{(y-y_m)^2}{2}$ $\frac{n^2}{2}(\Delta y)^2$	④ $W_{z,m}^*$	⑤ $\left(\frac{\partial W_z^*}{\partial y}\right)_m$	⑥ $\left(\frac{\partial^2 W_z^*}{\partial y^2}\right)_m$	⑦ W_z^* ④+②⑤+③⑥	⑧ $W_{y,m}^*$	⑨ $\left(\frac{\partial W_y^*}{\partial y}\right)_m$	⑩ $\left(\frac{\partial^2 W_y^*}{\partial y^2}\right)_m$	⑪ W_y^* ⑧+②⑨+③⑩	⑫ W^* $\sqrt{⑦^2 + ⑪^2}$	⑬ ρ^* From ⑫ and fig. 5	⑭ $\rho^* W_z^*$ ⑦⑬	⑮ M^* $\int_{y_m}^{y} ⑭\, dy$	⑯ Blade y coordinate obtained for $M^* = \pm 0.5085$
$4\Delta y_p$	1.5383	0.53333	0.14222	-------	--------	-------	.91263	--------	-------	--------	-0.64165	1.11562	1.0272	0.93745	0.65975	-------
$3\Delta y_p$	1.4050	.40000	.08000	-------	--------	-------	1.08354	--------	-------	--------	- .59989	1.23852	1.0116	1.09611	.52412	1.39070
$2\Delta y_p$	1.2717	.26667	.03556	-------	--------	-------	1.25759	--------	-------	--------	- .61018	1.39780	.9910	1.24627	.36783	-------
Δy_p	1.1383	.13333	.00889	-------	--------	-------	1.43481	--------	-------	--------	- .67250	1.58459	.9636	1.38258	-------	-------
y_m	1.0050	--------	-------	1.61516	-1.36449	0.17715	1.61516	-0.78687	1.05297	-2.92758	- .78687	1.79664	.9285	1.49968	-------	-------
Δy_s	.9057	- .09933	.00493	-------	--------	-------	1.75157	--------	-------	--------	- .90589	1.97196	.8973	1.57168	-------	-------
$2\Delta y_s$	.8063	- .19867	.01973	-------	--------	-------	1.88974	--------	-------	--------	-1.05382	2.16370	.8603	1.62574	-.31165	-------
$3\Delta y_s$	.7070	- .29800	.04440	-------	--------	-------	2.02964	--------	-------	--------	-1.23064	2.37359	.8176	1.65943	-.47499	.68679
$4\Delta y_s$	.6077	- .39733	.07894	-------	--------	-------	2.17130	--------	-------	--------	-1.43635	2.60339	.7684	1.66843	-.64051	-------

2223

TABLE V - RESIDUALS OBTAINED IN COMPRESSIBLE SOLUTION OF THIRD EXAMPLE

y \ z	0.18	0.36	0.54	0.72	0.90	1.08	1.26	1.44	1.62	1.80
1.176		0.2093	0.7716	-0.0361	-0.2726	0.0989				
1.029	-1.2212	- .1610	.3052	.3007	.1913	.1127	0.0752	-0.4316	-0.0797	
.882	-1.0128	- .2084	.1641	.0091	.1671	.0279	- .3206	.2230	- .2538	-0.2408
.735	- .3648	.2068	- .0093	- .1896	- .1197	- .1168	- .2642	- .1612	- .1942	.3271
.588	.1086	.2642	.0211	- .0233	.2706	.0586	.5123	.1244	.1099	.4335
.441	- .3708	- .3869	.6299	- .1013	- .1494	.0229	- .0189	- .9797	.0698	.2336
.294	- .5373						- .0003	.2631	- .2363	- .3507
.147									- .4918	.0368
0										.3491

TABLE VI - ESTIMATED PERCENTAGE ERROR IN $\partial\psi/\partial y$ or ρW_z

y \ z	0.18	0.36	0.54	0.72	0.90	1.08	1.26	1.44	1.62	1.80
1.176		-0.01005	-0.01217	0.01223	0.01342	0.00119				
1.029	-0.00022	- .00771	- .01115	.00081	.00779	- .00128	0.01148	0.02231	-0.00597	
.882	.01599	.00644	- .00541	- .00830	- .00524	- .00392	- .00599	.00498	- .00226	0.01664
.735	.01997	.00785	- .00228	- .00051	.00162	.00049	.01381	- .00177	.00691	.01366
.588	- .00010	- .00952	.00941	.00128	- .00043	.00210	.00393	- .01441	.00496	- .00190
.441	- .00107	- .01544	.01228	- .00268	- .01121	- .00199	- .00795	.00236	- .00650	- .01598
.294	- .00015						.00437	.04036	- .01052	- .00394
.147									- .00432	.01379
0										.00555

NACA

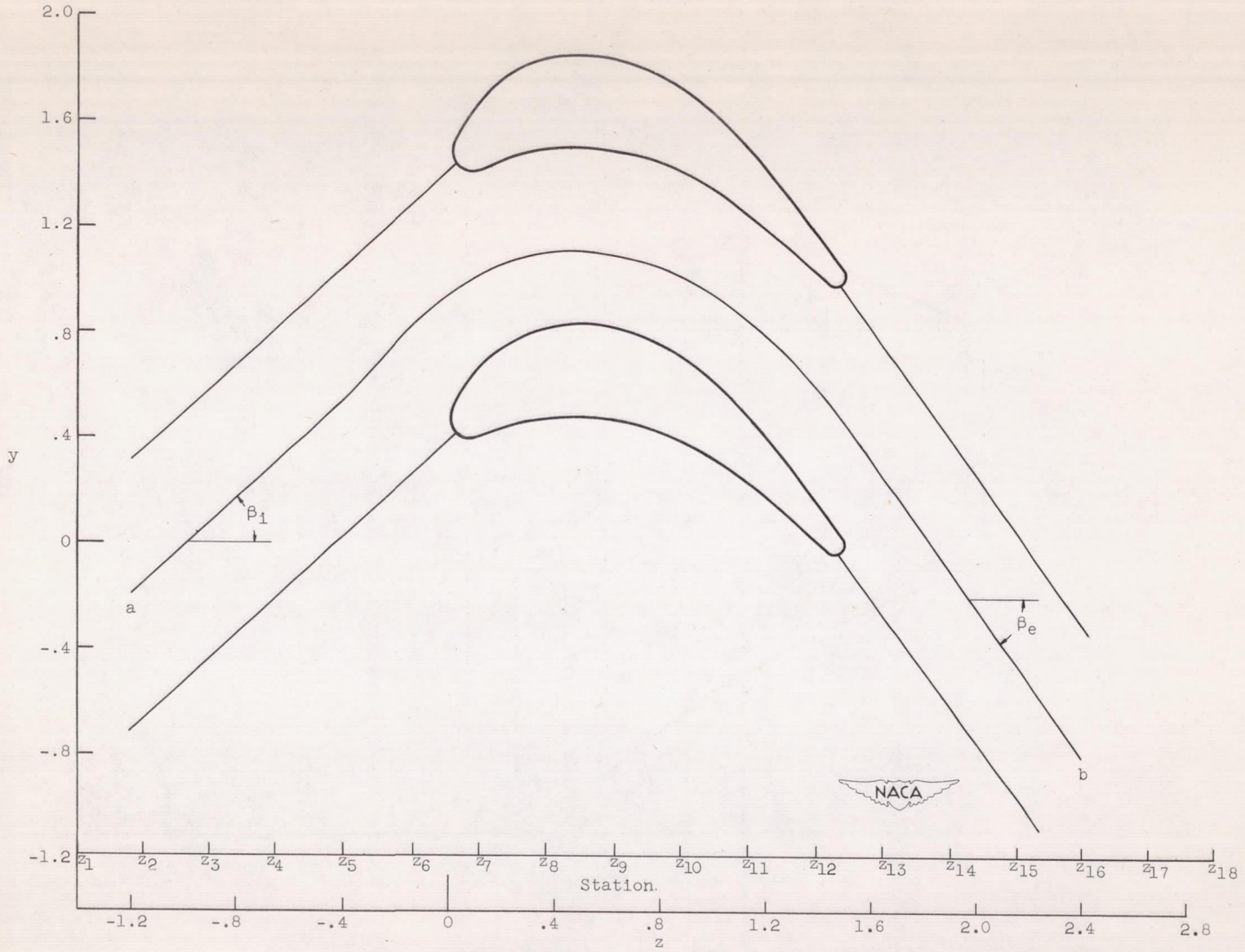


Figure 1. - Mean streamline, inlet and exit angles, and z-stations.

2223

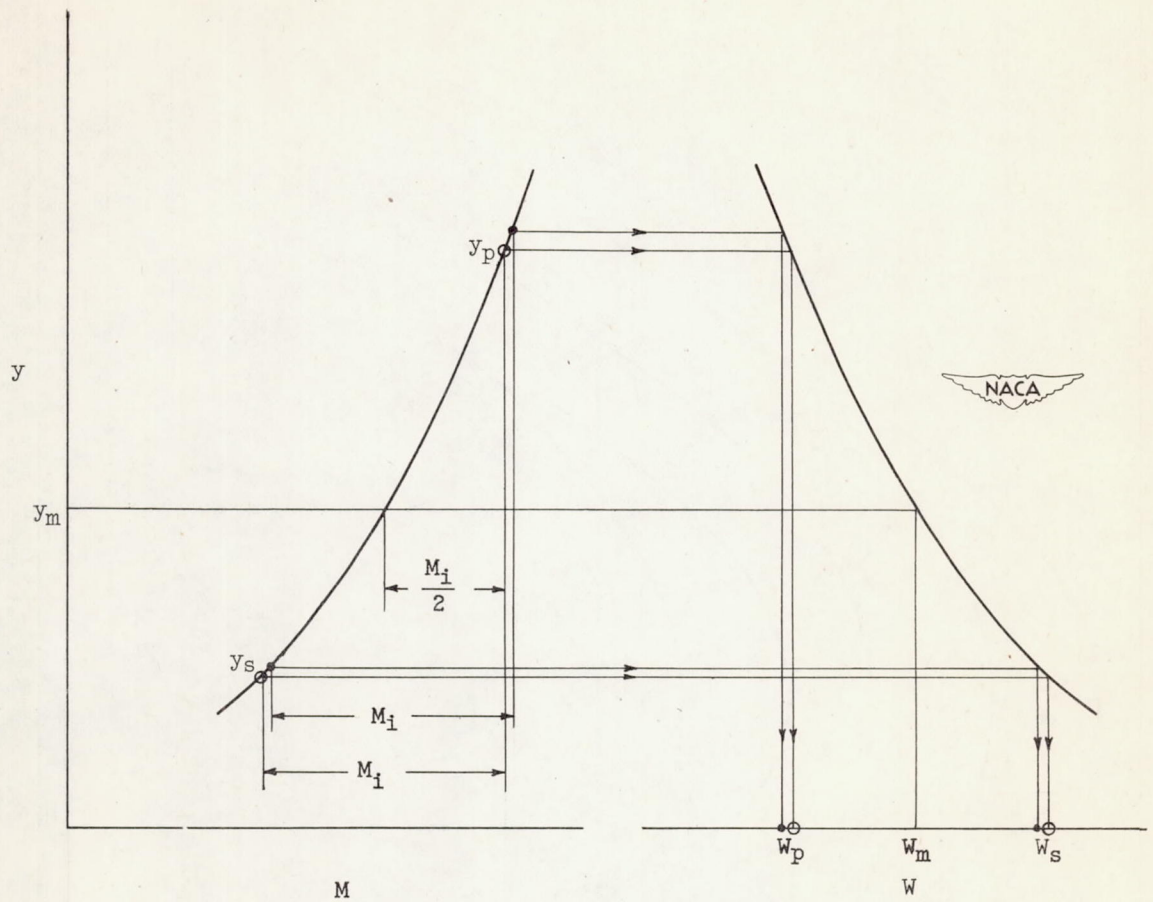


Figure 2. - Determination of blade coordinate and velocity on blade.

2223

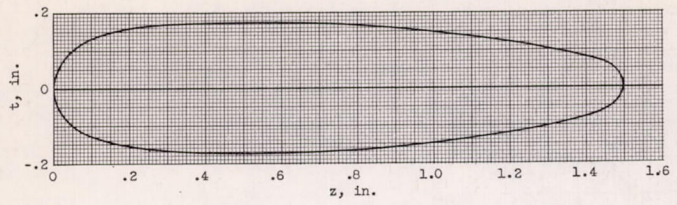


Figure 3. - Blade-thickness distribution.

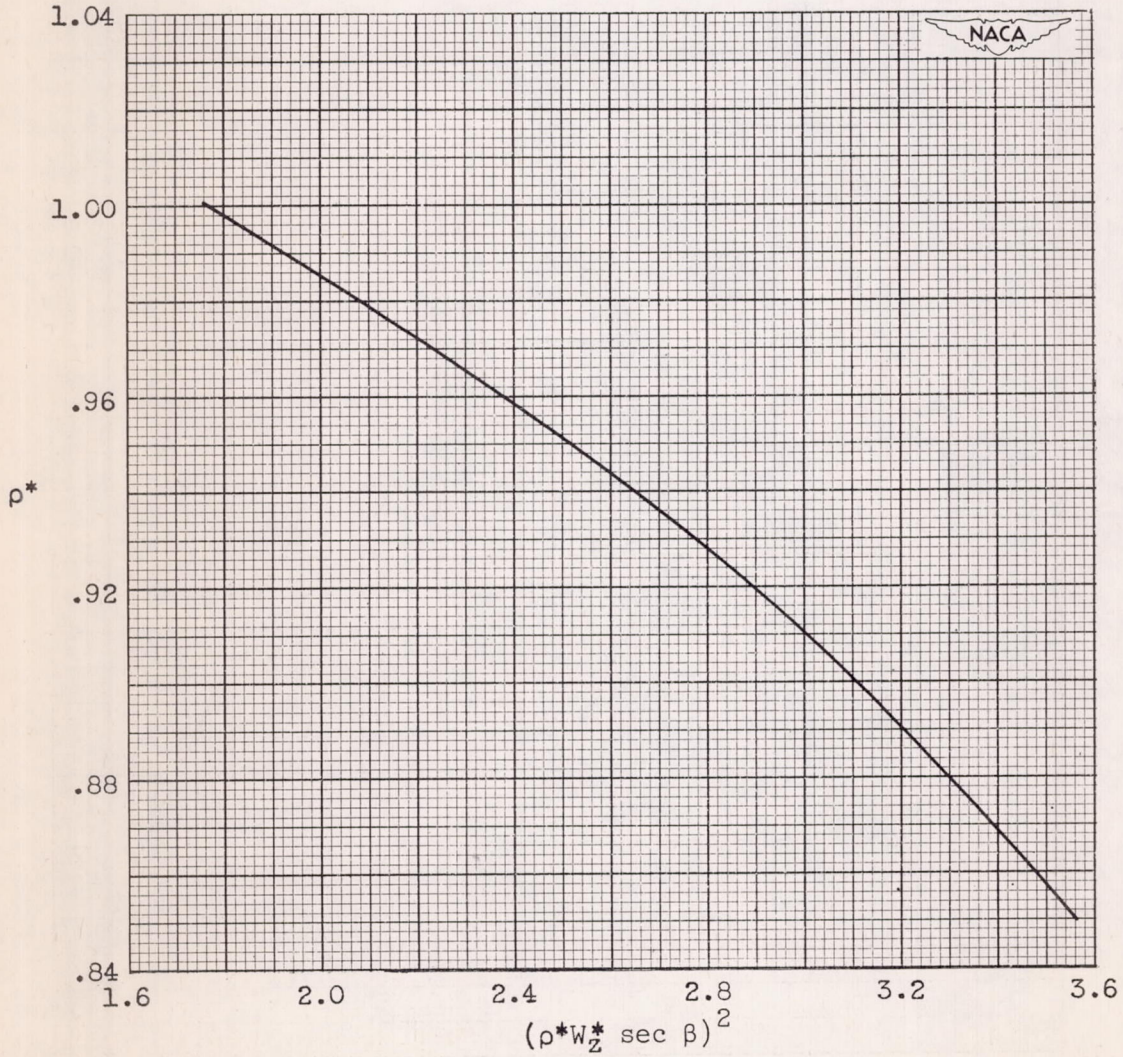


Figure 4. - Variation of ρ^* with $(\rho^* W_z^* \sec \beta)^2$ in accordance with equation (12b).

2223

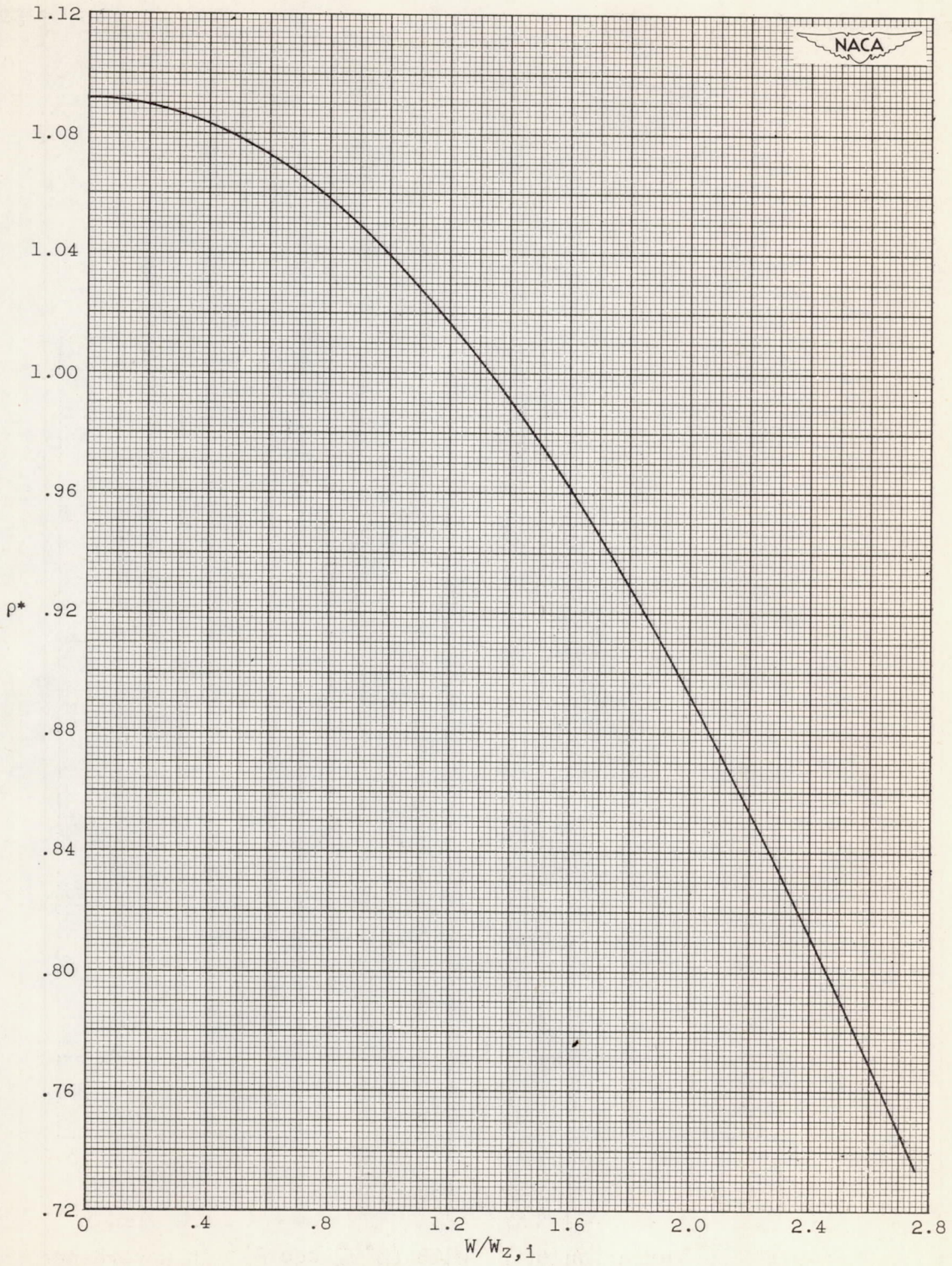


Figure 5. - Variation of ρ^* with $W/W_{z,i}$ in accordance with equation (12).

2223

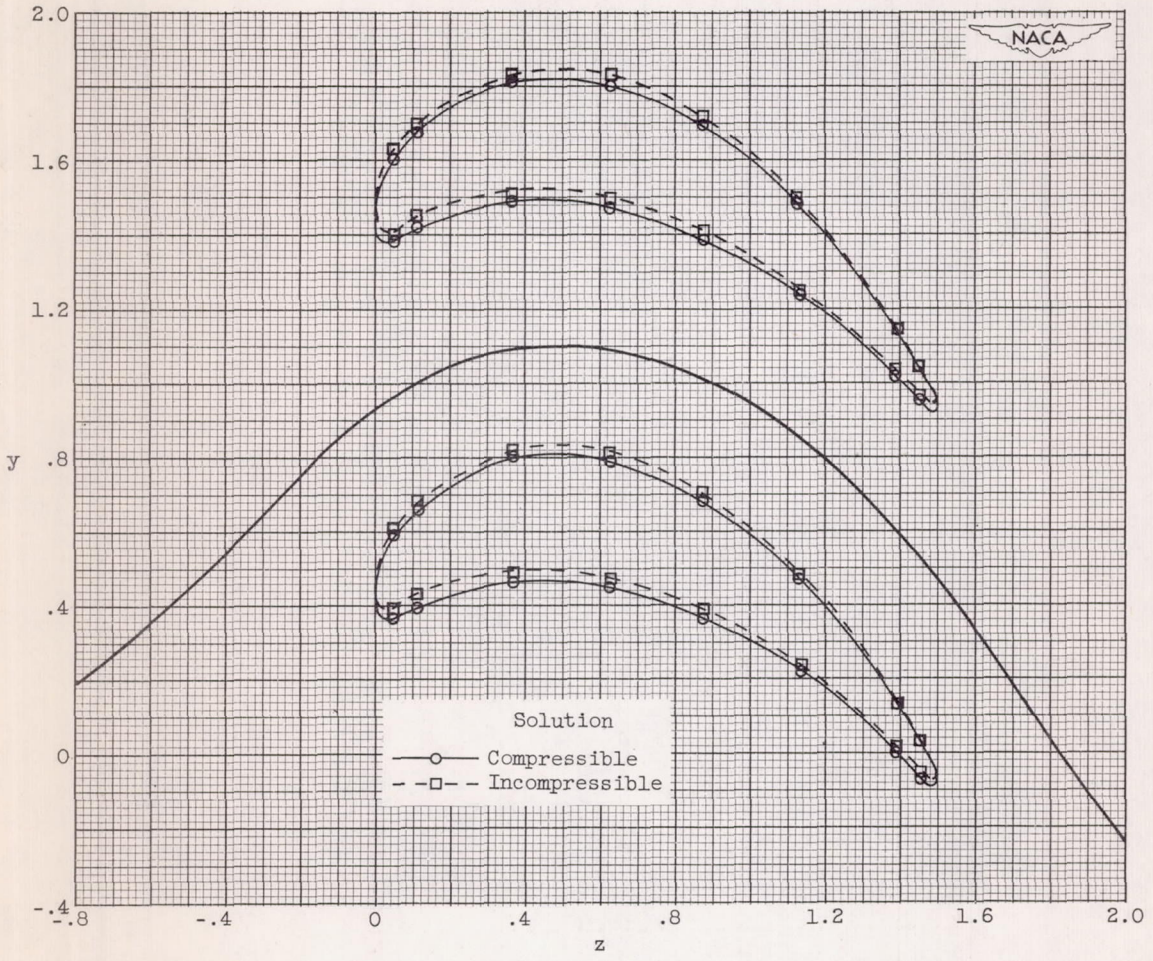


Figure 6. - Inverse solutions for compressible and incompressible flows.

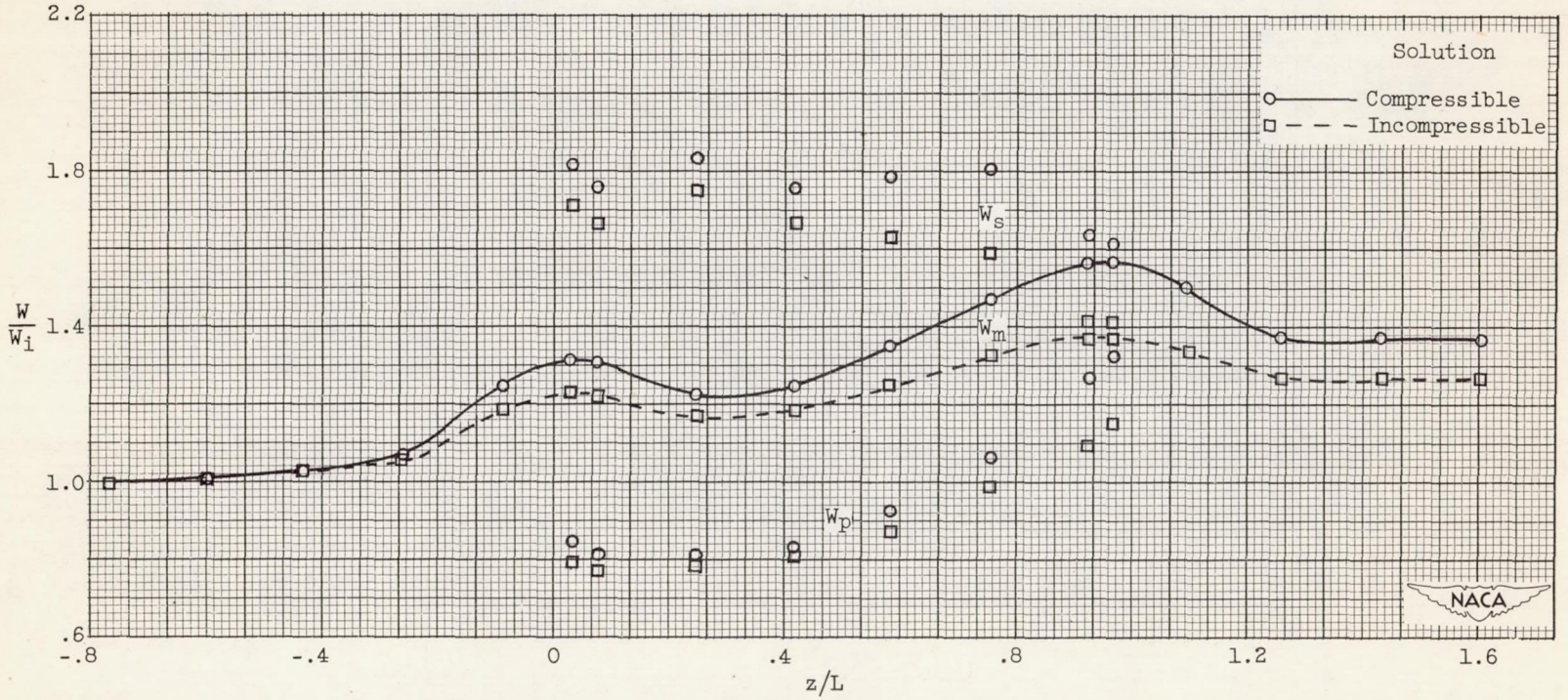


Figure 7. - Velocities on blade surfaces and mean streamline obtained in inverse solutions.

2223

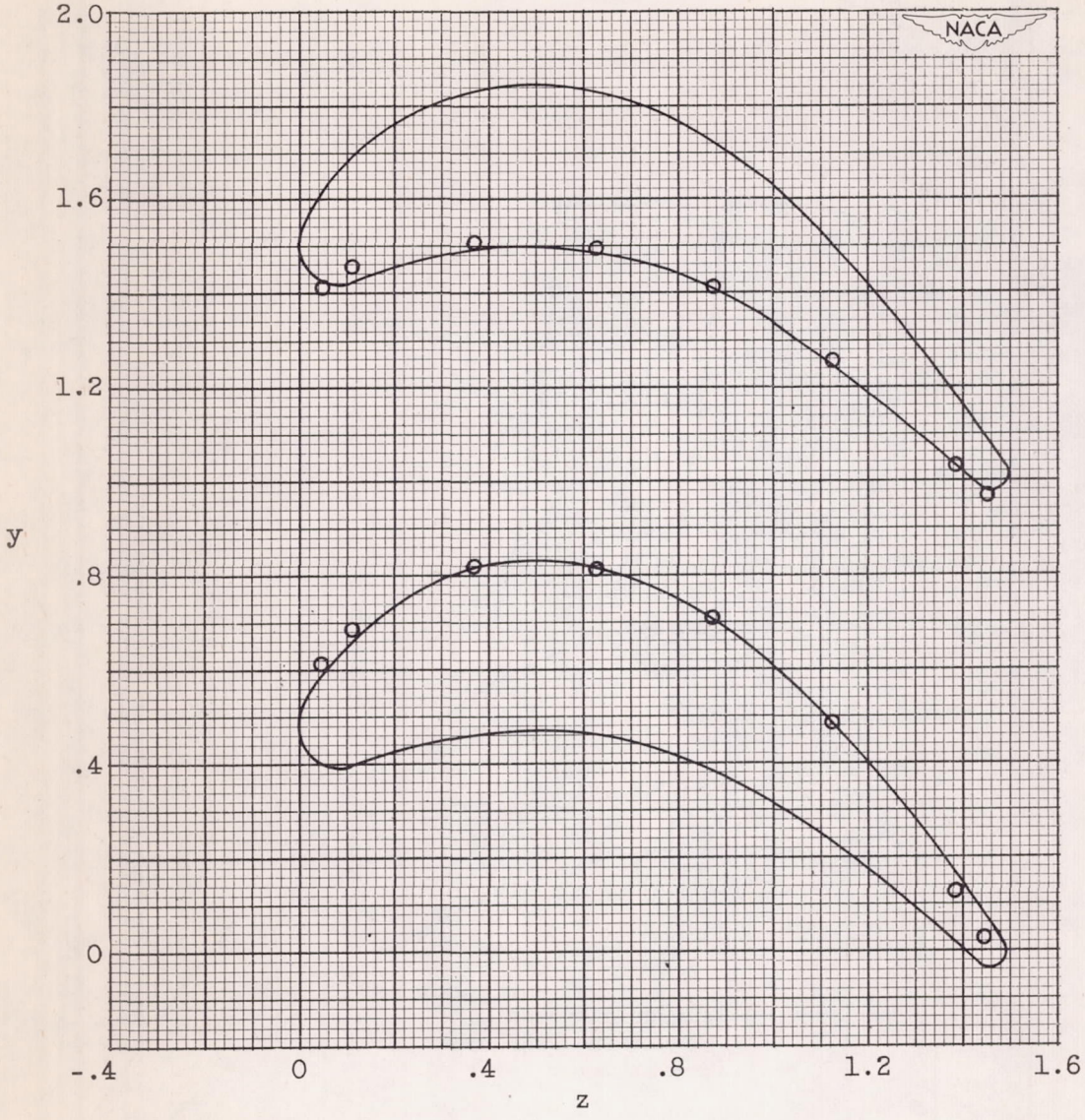


Figure 8. - Comparison of incompressible solution with original blade.

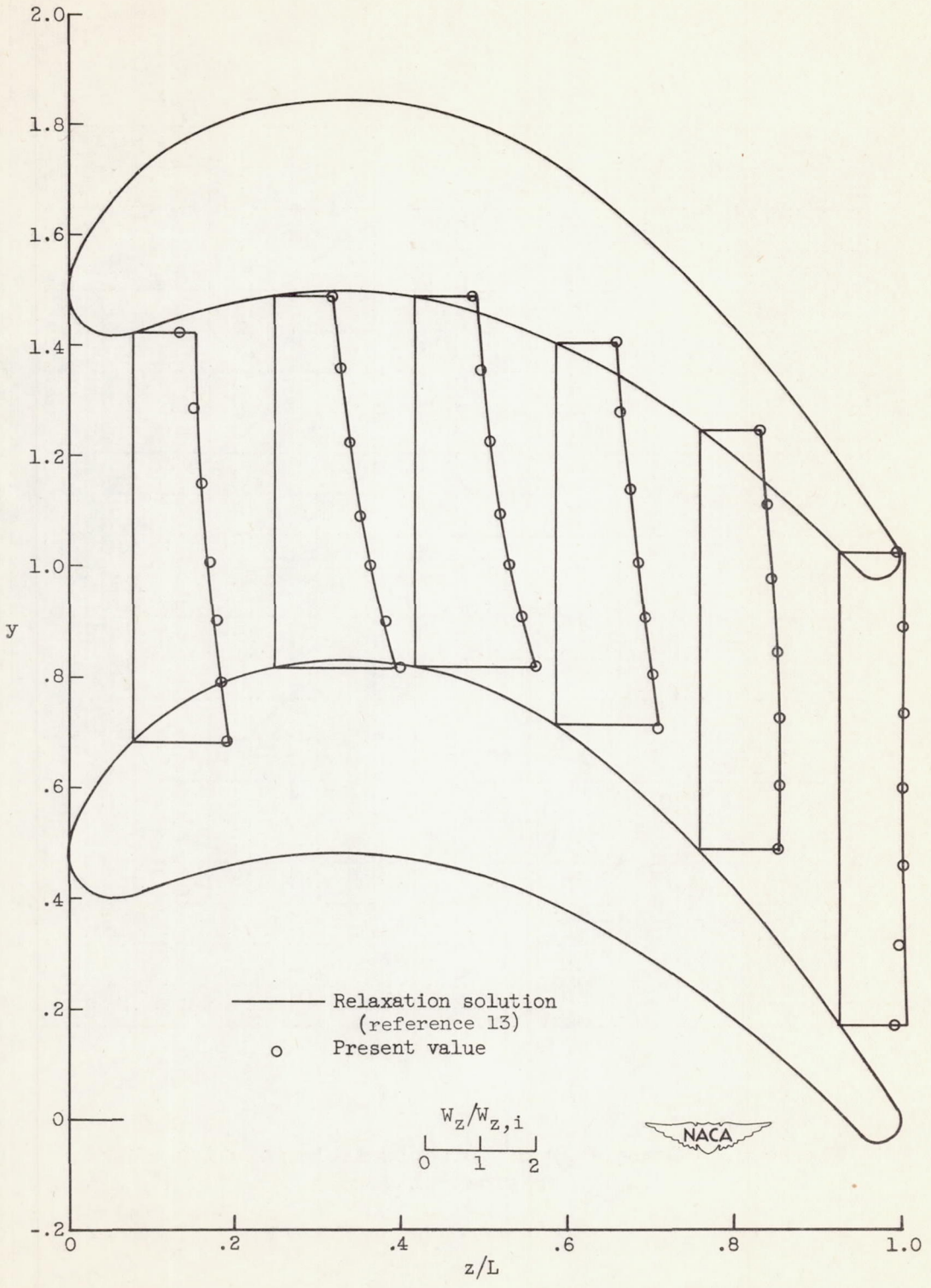


Figure 9. - Comparison of axial velocities. Vertical lines are stations. Using scale, read horizontal distance from station to corresponding curve to obtain velocity.

2223

2223

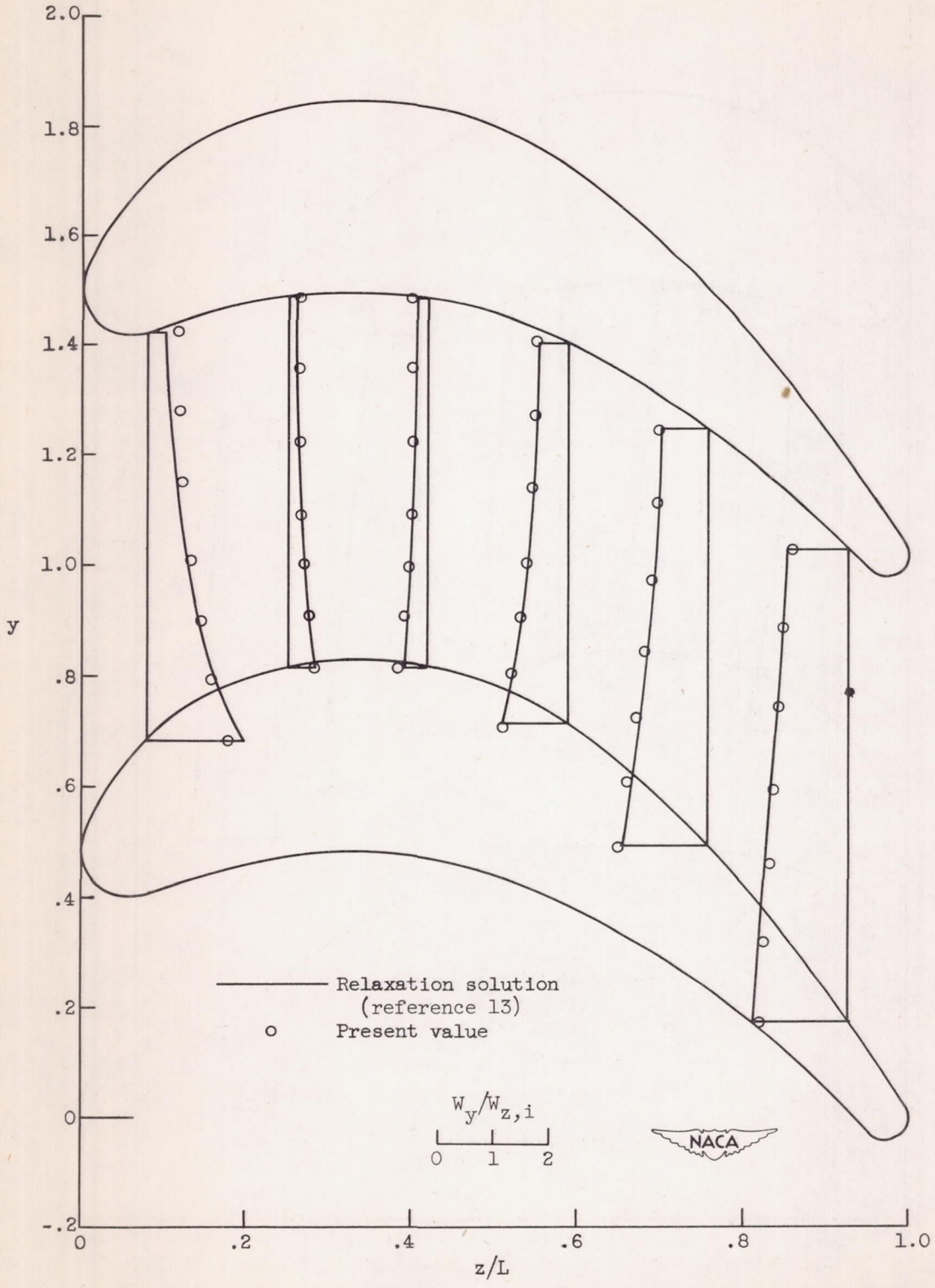


Figure 10. - Comparison of tangential velocities. Vertical lines are stations. Using scale, read horizontal distance from station to corresponding curve to obtain velocity.

2223

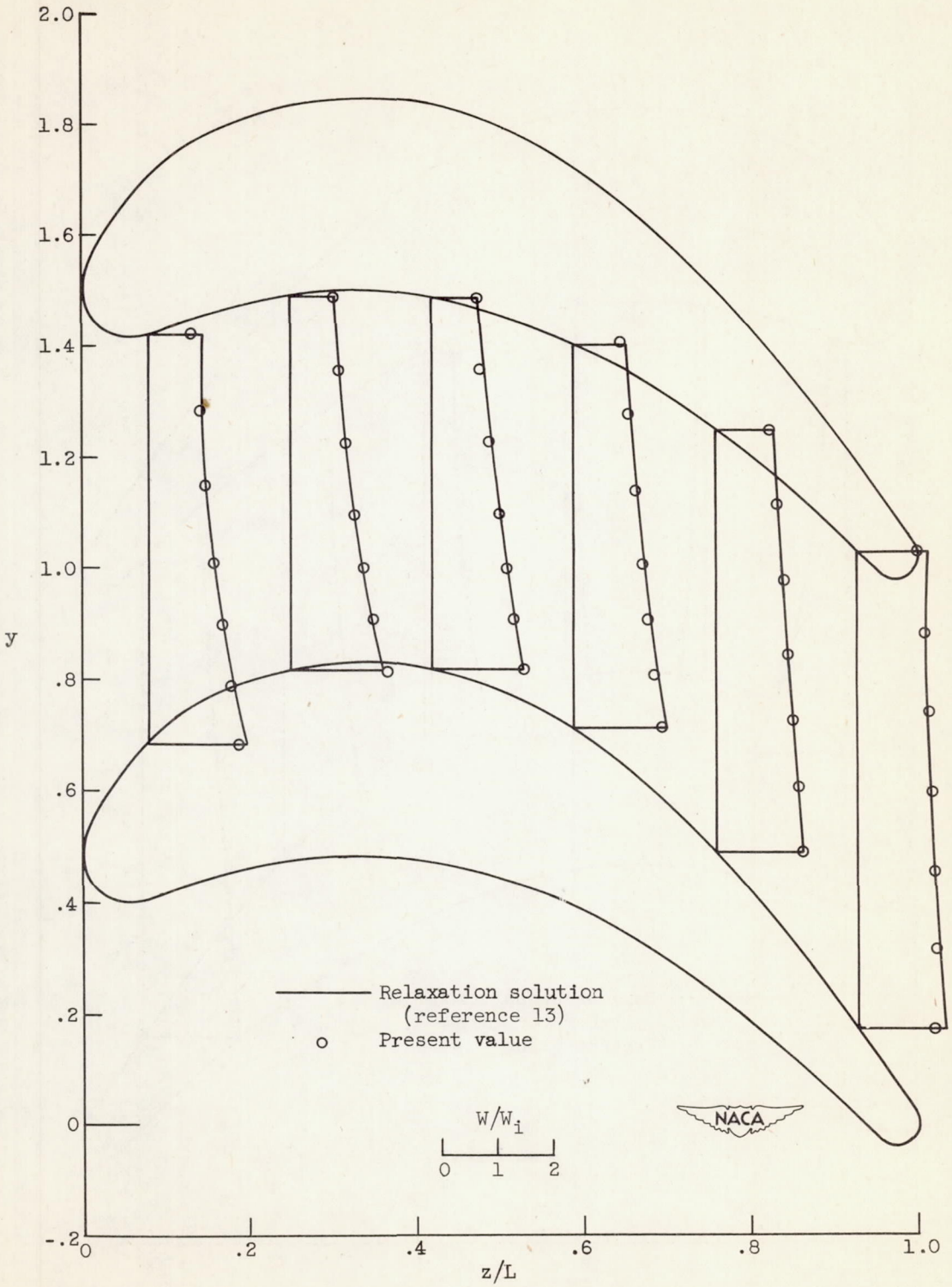


Figure 11. - Comparison of resultant velocities. Vertical lines are stations. Using scale, read horizontal distance from station to corresponding curve to obtain velocity.

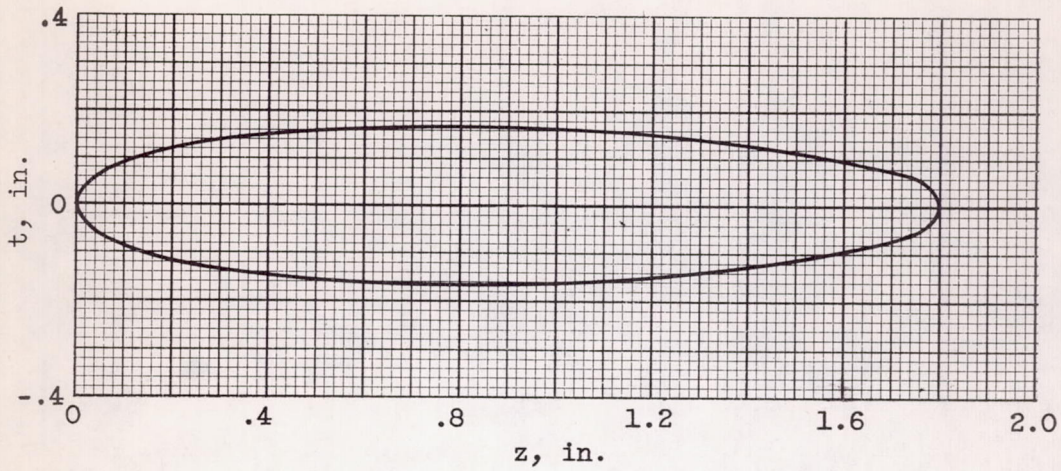


Figure 12. - Blade-thickness distribution.

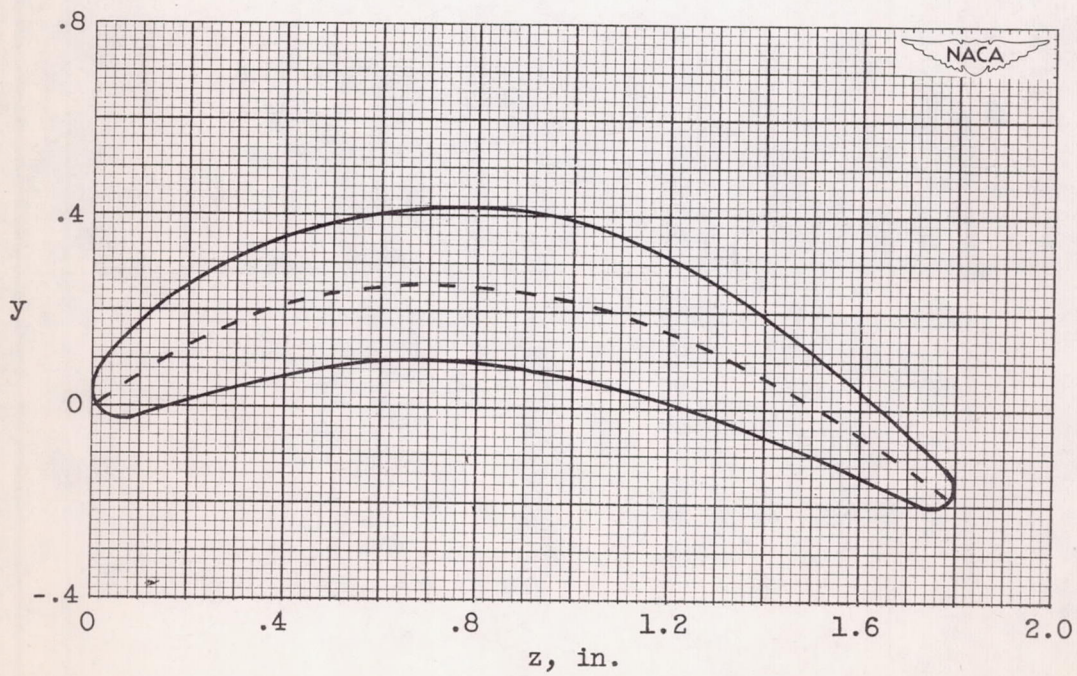


Figure 13. - Desirable mean blade line and corresponding blade shape.

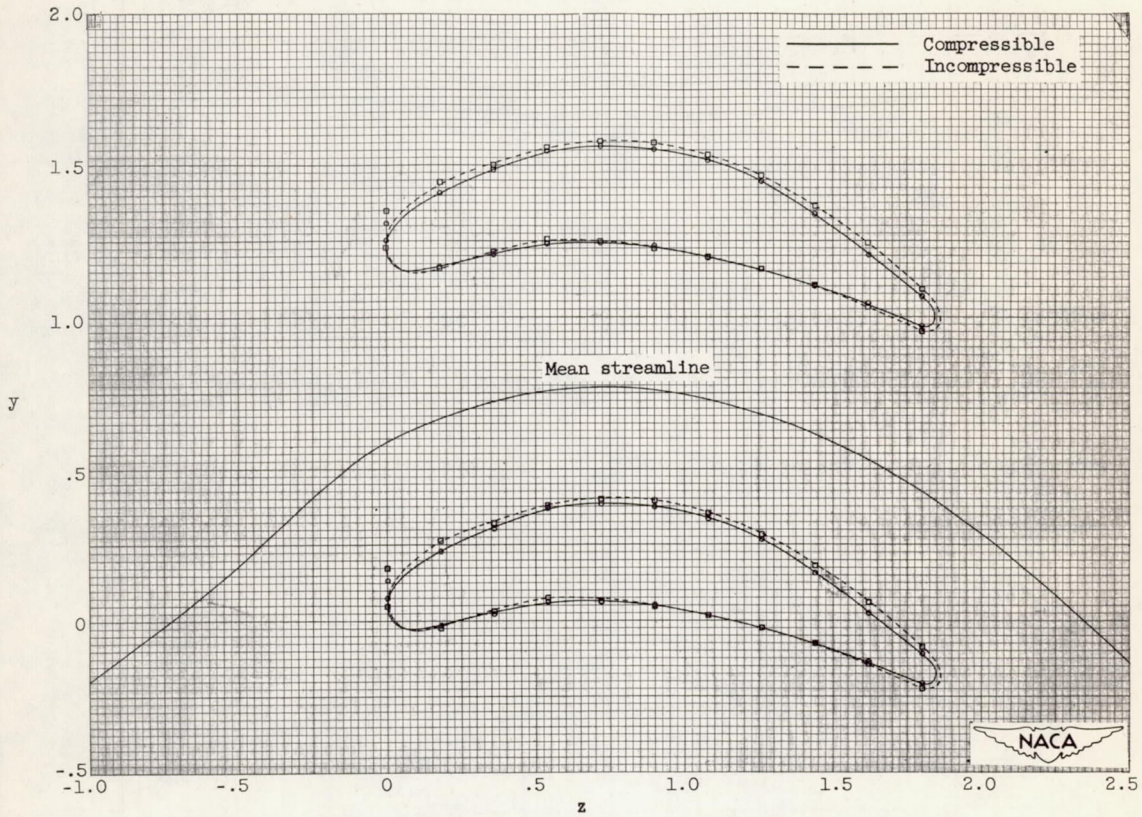


Figure 14. - Mean streamline shape and resultant blades.

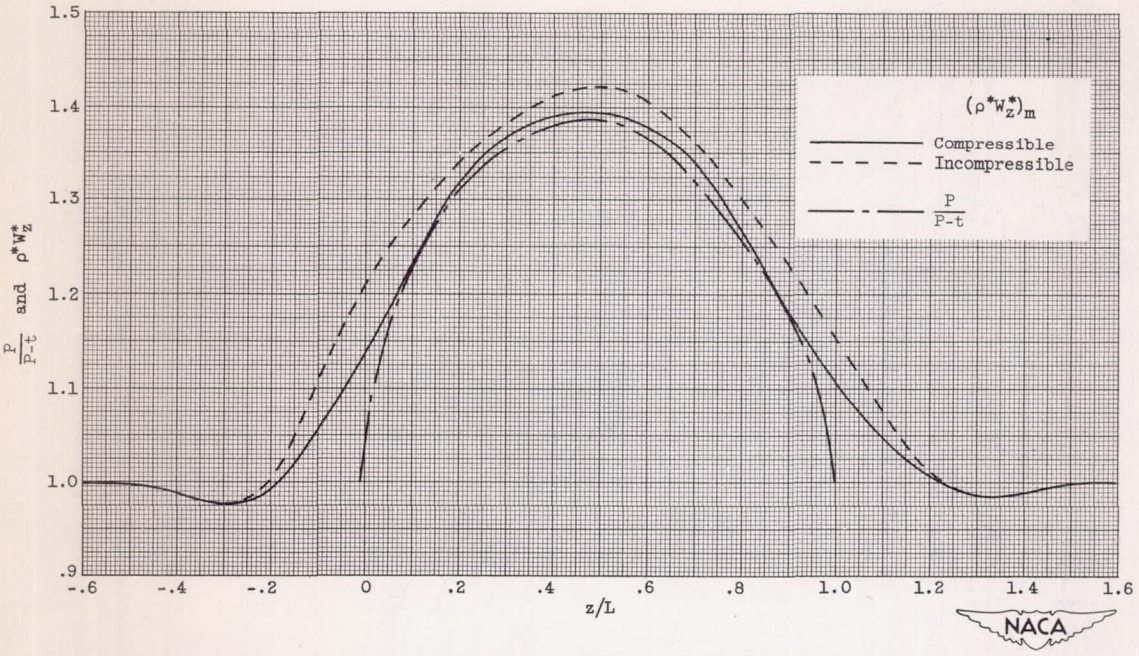
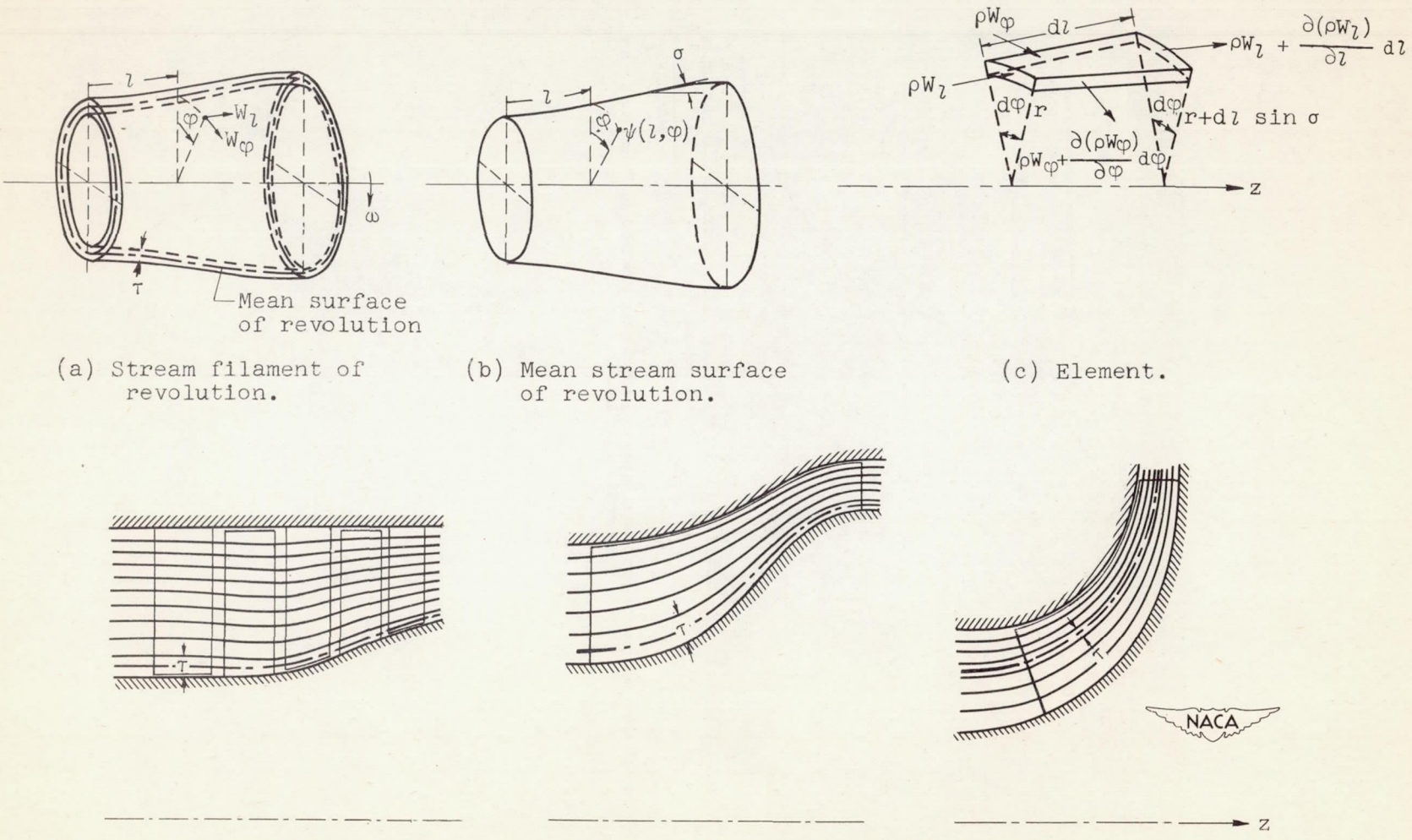


Figure 15. - Channel width ratio and specific mass flow along mean stream line used in incompressible and compressible solutions.



(a) Stream filament of revolution.

(b) Mean stream surface of revolution.

(c) Element.

(d) Applications to axial-flow, mixed-flow, and radial-flow turbomachines.

Figure 16. - Flow on arbitrary surface of revolution and stream filament of revolution.

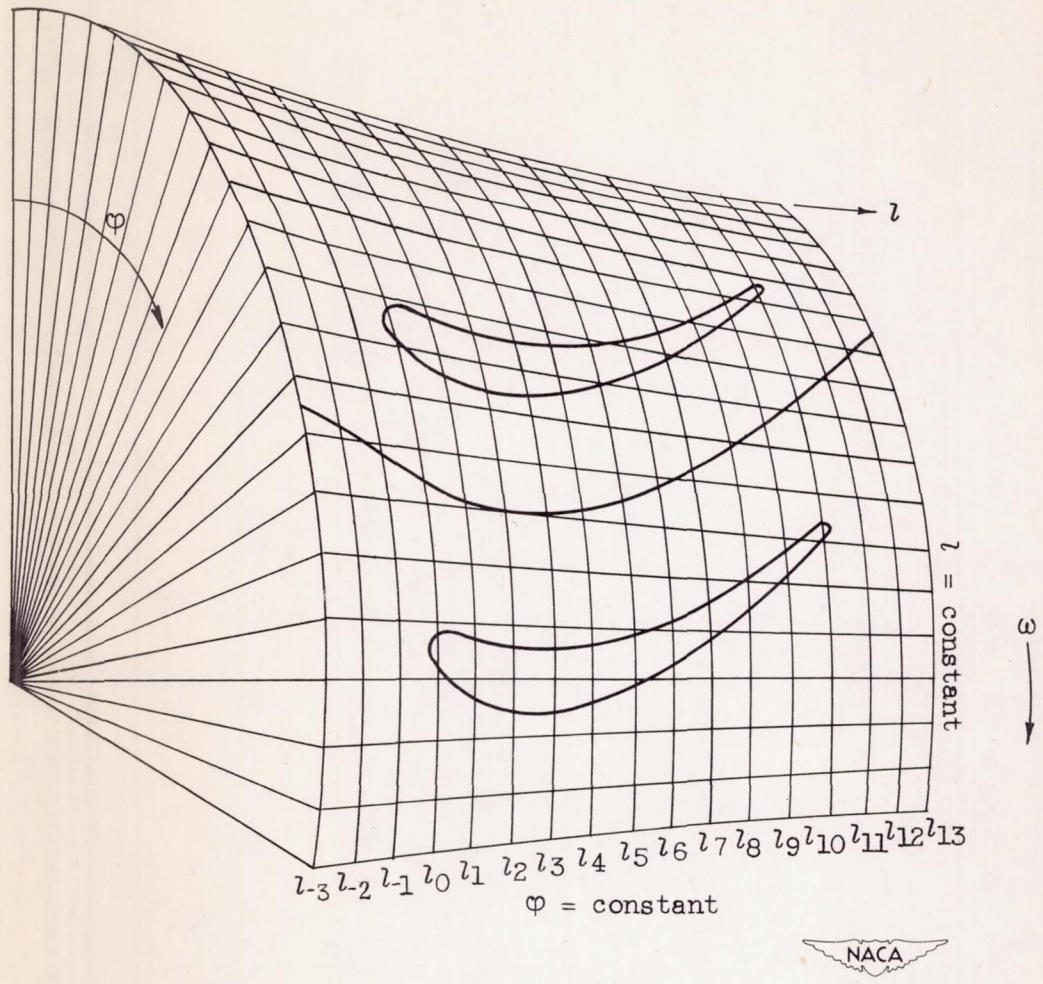


Figure 17. - Blade section on arbitrary surface of revolution.